# RARE EARTH ION PAIR ABSORPTION AT LOW CONCENTRATIONS IN LANTHANUM TRICHLORIDE

by

JOEL HERMAN BLATT

A DISSERTATION

Submitted in partial fulfillment of the requirements for the degree of Doctor of Philosophy in the Department of Physics in the Graduate School of the University of Alabama

UNIVERSITY, ALABAMA

1970

## ACKNOWLEDGEMENT

The author wishes to thank Professor John F. Porter, Jr. for his support and encouragement throughout this work. He is also indebted to Professor J. Edwin Rush, Jr. for his assistance in suggesting the problem. The author is particularly grateful to Professor J. G. Castle, Jr., whose advice and analysis proved invaluable during the investigation, as well as in the preparation of the manuscript. He also wishes to thank Dr. John D. Stettler for several helpful discussions and Mrs. Eugenia Bledsoe for her infinite patience in typing the many drafts of the manuscript.

This work was supported by the U. S. Army Missile Command under Contract DA-AH01-69-C-1096 and by the U. S. Army Research Office-Durham under Contract DA-HC-04-67C0068.

TABLE OF CONTENTS

## LIST OF FIGURES

LIST OF TABLES

# CHAPTER I

# INTRODUCTION

## 1. Purpose and Scope of Work

The study of energy transfer between excited states of ions in crystals has been stimulated in recent years by the advent of the solid state laser and by efforts to increase its efficiency and to modify the wavelength and coherence of its output. A more fundamental reason for the continuing interest in energy transfer is the possibility of gaining an insight into the mechanisms by which the ions interact with the lattice and with each other. Many of these processes imply the existence of interactions whose long range and concentration dependence have yet to be satisfactorily explained.

The primary purpose of this investigation was to establish the occurrence of absorption of a single photon by a pair of rare earth ions at low concentrations in $LaCl_3$. Previous rare earth two ion absorptions have only been reported in high concentration samples.[1,2]

The technique used to establish the existence of the two ion absorption process must be able to distinguish between the weak absorption expected for ion pairs and the strong absorption due to

single ions. Thus a primary requirement for the ions chosen is that they have energy levels such that the sums of pairs of individual ion energy levels do not lie in a region including any single ion levels.

The ions chosen for this investigation were $Pr^{3+}$ and $Ho^{3+}$, since they had well determined energy level schemes in $LaCl_3$ which met the above requirement. $Nd^{3+}$ was also included since it was known to be present as an impurity.

The scope of work covered in this investigation included studies of the fluorescence spectra of $Ho^{3+}$, $Pr^{3+}$, $Ho^{3+} + Pr^{3+}$, and $Ho^{3+} + Nd^{3+}$ dilutely doped in $LaCl_3$ at $4.2^{\circ}K$ under approximately 32,000 $cm^{-1}$ excitation. Other excitation energies were used to establish the identity of the observed fluorescence. In addition, studies of the photographic absorption spectra of the above crystals, and of the excitation spectra of the prominent fluorescence lines observed were included in the work. Finally, an analysis of the experimental results obtained and recommendations for future work are included.

## 2. Review of Energy Transfer Processes in Crystals

### a. Radiative Transitions

The mechanism of energy transfer due to radiative transitions between electronic energy levels is quite well known. For the trivalent rare earths diluted in anhydrous $LaCl_3$, fluorescence from an ion at a given level normally is observed if an energy gap of greater than 1000 $cm^{-1}$ exists between it and the next lowest level.[3] Although parity forbids electric dipole transitions between the levels of the $4f^n$ configurations, forced electric dipole and magnetic dipole transitions have been observed to take place.

The forced electric dipole transition is observed when the crystal field at the rare earth ion site lacks a center of symmetry. The lack of symmetry causes the electronic wave function to have a mixed parity, although it is still predominately of one parity, determined by the number of 4f electrons. The admixture of opposite parity in the wave function is quite small due to the small fraction of the total field that is noncentrally symmetric, but is sufficient to allow these forced electric dipole transitions to account for the majority of the observed crystal lines.

Weak magnetic dipole transitions are observed for many lines, in addition to the allowed lines which lie in the infrared. Their presence has been explained by the mixing of parts of

various multiplets in a given state due to intermediate coupling, and by the presence of nondiagonal elements in J due to J-mixing in the crystal field.[4]

b. Multiphonon Emission

As has been mentioned, rare earth energy levels separated from adjacent lower levels by energy gaps of less than approximately 1000 $cm^{-1}$ are not observed to radiate in $LaCl_3$. In fact, according to the work of Barasch,[5] for energy gaps of less than 1000 $cm^{-1}$, transitions characterized by multiphonon emission dominate, while for gaps larger than 4000 $cm^{-1}$, the radiative transitions are the primary means of de-excitation. Kiel has shown that at its maximum, the nonradiative transition probability can be comparable to the radiative transition probability at its maximum.[6] The large size of the nonradiative transition probability is due to the high density of final states in the phonon distribution function. Since the phonon spectrum cut-off in $LaCl_3$ is on the order of a few hundred $cm^{-1}$, the nonradiative decay of levels separated by 1000 $cm^{-1}$ must involve several phonons. The exponential dependence on the energy gap of the multiphonon transition rate can be demonstrated by examining the requirement for convergence of the orbit-lattice perturbation

expansion, and has been experimentally verified by Riseberg and Moos,[7] from 4.2°K to approximately 350°K.

c. Multiple Ion Processes

Radiationless transfer of energy from one ion to another in a crystal lattice by means other than multiphonon processes has received considerable attention recently, both from experimental and theoretical viewpoints. In most of the mechanisms to be discussed below, a phonon may be emitted or absorbed to conserve energy.

The theory of sensitized luminescence has been extensively discussed recently by Förster,[8] Dexter,[9, 10] Dow,[11] and Birgeneau.[12] In a classic paper, Dexter[9] considered the energy transfer mechanism whereby an activator impurity emits light after the absorption of light by another impurity, the sensitizer. The mechanisms proposed are, in order of increasing strength, the exchange interaction due to the actual overlap of the electronic wave functions, the overlapping of the dipole field of the sensitizer with the quadrupole field of the activator, and the overlapping of the dipole fields of both the sensitizer and the activator. These mechanisms were later extended to cover quadrupole-dipole and quadrupole-quadrupole interactions.[10]

Whereas Förster[8] originally only considered resonant transfer involving allowed transitions in both the activator and sensitizer with dipole-dipole coupling between them, Dexter extended the theory to cover forbidden transitions in either the activator, or sensitizer, or both. He was able to show that actual overlap of the sensitizer and activator wave functions is unimportant whenever strong electric dipole transitions are allowed, but that for magnetic dipole and higher order transitions, the exchange interaction due to overlap of the electronic wave functions becomes important. Resonance energy transfer is defined here as the process where a local impurity is excited and the stored energy jumps to a nearby impurity, not necessarily of the same species. The perturbation that enables the energy transfer to take place is the Coulomb interaction between the outer electrons and core of the two impurity centers. This Coulomb interaction is expanded in a Taylor series about the vector joining the activator and sensitizer, and then separated into terms corresponding to the various multipole interactions.

Dow[11] considered the resonance energy transfer problem from the standpoint of a many particle system with a detailed analysis of the nature of the excitation migration. He was able to show that the

Förster-Dexter (F-D) theory is valid for energy transfer only for very low impurity concentrations. In the regions of its validity, the approximations of the F-D theory were shown to be related to the more complicated effects of the detailed model. Dow also points out that for concentrations higher than 0.001, 0.1, 0.003, 0.03, and 1%, for dd, dq, qd, qq, and exchange transfer interactions, multiple scattering of the excitation must be taken into account and the simple F-D theory is not valid. The transition rate for a given process was shown to be dependent on the distance between activator and sensitizer. Dow showed that the transition rate could be unambiguously converted into a dependence on activator concentration for concentrations lower than the above values.

Imbusch[13] has measured the concentration dependence of the energy transfer between single chromium ions and exchange coupled pairs of chromium ions in ruby and concludes from the experimental results that the quadrupole-quadrupole (qq) coupling is responsible for the process. However, in a recent paper, Birgeneau[12] questions the validity of the technique of assigning a mechanism of interaction based on studies of the concentration dependence of energy transfer processes.

Dexter[14] has discussed the interactions responsible for, and the probability of, a process involving the absorption of a single photon of incoming light by a pair of neighboring ions in a crystal. First order perturbation theory was used to generate total wave functions from the first order single ion functions using the Coulomb interaction as the perturbation. He then considered the interaction of the electrons with the incoming electromagnetic field as the perturbation which couples the total states with the excited states. Dexter accomplished this coupling by summing over virtual excited states. The normal optical matrix elements which connect the ground and excited states do not appear explicitly, but do appear coupling the ground to the virtual states. The Coulomb interaction is then expanded in multipoles, and the magnitude of the transition matrix element can be evaluated in terms of the radiation strength and the separation of the two ions. Finally, he concluded that in the case of the rare earth ions, due to the shielded inner electrons, the exchange interaction should be of negligible importance except in two cases: First, if the two ions are nearest neighbors and the wave functions are not well localized, and second, if the first few terms of the multipole expansion are made to vanish because of the selection

rules governing atomic transitions.

3. Previous Experimental Work on Multiple Ion Processes

a. Ion Pair Relaxation

If the energy gap between an excited level and the next lower level is on the order of the energy gap separating the ground and first excited levels, then an energy transfer process called ion pair relaxation can take place. In this process, an ion at the upper excited level can decay to the next lower level by exciting another ion from the ground level to the first excited level. Slight energy mismatches may be compensated for by the emission or absorption of a phonon.

This process was first reported for similar ions by Varsanyi and Dieke.[1] They found that for several sets of levels in $Er^{3+}$ diluted in $LaCl_3$, fluorescence was observed from ions at levels approximately 6700 $cm^{-1}$ below the pumped levels. The energy difference between these two levels is slightly larger than the difference between the ground level and the first excited level $(6690\ cm^{-1})$, and they theorized that ions in the upper state were relaxing to the lower state by exciting other ions up from the ground to the first excited

state.

A similar process was reported by DeShazer and Dieke[15] for $Eu^{3+}$ in $LaCl_3$. In this case, no fluorescence was observed from ions excited to the $^5D_3$ level, but strong fluorescence was observed from ions at the $^5D_2$ and $^7F_4$ levels. Here, the energy difference $^5D_3 - ^5D_2$ is only 2 $cm^{-1}$ larger than the energy difference $^7F_4 - ^7F_0$ (ground level).

Dieke and Pandey[16] have also observed ion pair relaxation in $Ho^{3+}$: $LaCl_3$ from a number of levels. They found that the following pairs of levels all had a fairly good energy match for the energy gap between the ground and first excited state: $^3H_5 - ^5G_6$, $^5G_4 - ^5F_3$, $^5G_5 - ^5S_2$, and $^5F_3 - ^5F_5$. Porter[17] and Porter and Moos[18] were able to show that in $Ho^{3+}$: $LaCl_3$, ions at the $^5S_2$ level relax to the $^5I_4$ level only by a pair process involving transitions from the ground level $^5I_8$ up to the first excited level $^5I_7$.

The ion pair relaxation process has also been observed for dissimilar ions, both in high and low concentrations. In a series of papers, Peterson and Bridenbaugh[19-22] investigated the relaxation process of $Tb^{3+}$ in several lattices, by both pulsed lifetime and continuous fluorescence studies. They found that fluorescence was

quenched from certain $Tb^{3+}$ levels when an impurity ion had an energy level structure such as to allow a pair relaxation process to take place. The ions $Nd^{3+}$, $Eu^{3+}$, and $Ho^{3+}$ were found to possess this property for lattices containing $Tb^{3+}$. In one case, the rise time of the impurity ion fluorescence from the $Eu^{3+}$ level $^5D_0$ matched the decay time of the $Tb^{3+}$ fluorescence from ions at the $^5D_4$ level. They also studied the effects of impurities on the relaxation processes of $Nd^{3+}$ in Na:Gd:$WO_4$ and found the pair relaxation process to be operating especially with $Yb^{3+}$, but also for all other rare earths except $La^{3+}$, $Ce^{3+}$, and $Gd^{3+}$.[23] The latter investigation was carried out with all the rare earth dopants in dilute concentrations in the host lattices. A similar effect has been seen in $Eu^{3+}$:$Y_2O_3$ with $Nd^{3+}$ and other rare earth dopants by Axe and Weller.[24] In the case of the $Nd^{3+}$ ion, there are six levels that match energy with transitions from the $Eu^{3+}\left(^5D_0\right)$ level.

Both Murphy, et al.[25] and Kiss[26] have investigated the transfer of energy from $Cr^{3+}$ ions to $Nd^{3+}$ ions in $LaAlO_3$, with the latter establishing that the energy transfer occurs between the $^2E$ state of $Cr^{3+}$ and the $^4F_{3/2}$ state of $Nd^{3+}$.

By studying optical line widths and line shapes, Yen, et al.[27]

were able to show that a fluorescence transition populating the $Pr^{3+}$ level $^3H_6$ in $LaF_3$ shifted from a Gaussian line shape due to strain broadening to a homogeneous broadening due to the change in lifetime as the $Nd^{3+}$ concentration was increased to 0.7% from 0%. This was traced to the depopulation of the $Pr^{3+}$ level $^3H_6$ to the level $^3H_5$ by a pair process with $Nd^{3+}\left(^4I_{9/2} \text{ to } ^4I_{11/2}\right)$.

Investigating rare earth activated CaS phosphors, Malhotra and Bhawalkar[28] have reported activation of Zr bands and $Dy^{3+}$ lines with increasing $Dy^{3+}$ concentration up to 0.006%, and then suppression of the Zr bands with higher $Dy^{3+}$ concentrations, which they relate to resonant transfer of energy from the Zr to the $Dy^{3+}$ ions. A similar process is indicated to be responsible by Belokrinitskii, et al.[29] for the reduction in the luminescence of $UO_2^{2+}$ glasses with $Nd^{3+}$ or $Eu^{3+}$ doping as a function of rare earth concentration, along with an increase in the rare earth fluorescence. These experiments, done at 300°K and 77°K indicate very little energy transfer between like ions, and practically no temperature dependence of the energy transfer process over the entire temperature range investigated.

All of the results so far discussed have dealt with ion pair relaxation processes in which there has been a close match in energy between

the upper levels of one ion and the ground and first excited states of the second ion. Slight mismatches in energy can be accounted for by the emission or absorption of a phonon.

The next pair process to be discussed was reported in $Cr^{3+}$ doped $EuAlO_3$ by van der Ziel and Van Uitert.[30, 31] They observed a process in which a $Cr^{3+}$ ion makes a transition from the $^2E_g$ to the $^4A_{2g}$ level, simultaneously exciting an $Eu^{3+}$ ion from the ground state to the $^7F_j$ level with the emission of a photon to conserve energy. This process was observed for j=1 through j=6. By means of relative intensity measurements, the authors identified the exchange interaction as the most probable coupling mechanism.

b. Ion Pair Absorption

If a single photon simultaneously excites two ions in a lattice, the process is called ion pair absorption. A process of this type would be detectable if there were no single ion energy levels in the range of the exciting photon, and if fluorescence transitions from the two simultaneously excited ions were subsequently observed. Ion pair absorption processes have previously been reported only in high concentration samples, with both similar and dissimilar ions taking part.

One of the earliest indications that an ion pair absorption could take place was found by Varsanyi and Dieke,[1] when they discovered that excitation in an area of no known energy levels produced fluorescence from ions at the $^3P_0$ level in 100% $PrCl_3$. They were able to show that if the excitation energy was equal to the sum of the energies of two $Pr^{3+}$ levels, one of which was the $^3P_0$ level, then fluorescence was produced corresponding to a $^3P_0$ transition. Subsequently, Dieke and Dorman[2] observed the absorption lines directly in 100% $PrCl_3$, although they were extremely weak, being smaller than absorption lines due to trace amount of $Nd^{3+}$ in the same sample. In their experiment, nearly all combinations of levels were observed in absorption, while Varsanyi and Dieke had only reported evidence for the excitation of ions to the $^3P_0$ level. Dieke and Dorman explained Varsanyi and Dieke's results as due to the extreme weakness of the fluorescence from all of the levels involved except the $^3P_0$ level in concentrated $PrCl_3$, as well as the fact that in concentrated $PrCl_3$, excitation of the nearby but higher levels $^3P_2$, $^3P_1$, and $^1I_6$ produces very little $^3P_0$ fluorescence, whereas in dilute solutions of $Pr^{3+}$ in $LaCl_3$, the $^3P_0$ fluorescence produced is very strong.

Evidence for the existence of ion pair absorption processes involving dissimilar ions was also reported by Margolis, Stafsudd, and Wong,[32] who investigated broad band fluorescence from a monochromatically excited sample of 100% $CeCl_3$ doped with 1% $Pr^{3+}$ at 77°K. Fluorescence from $Pr^{3+}$ was observed when the excitation energy was the sum of the $Ce^{3+}$ level $^2F_{7/2}$ and one of the $Pr^{3+}$ levels connected to the $^3P_0$ level by a multiphonon process. In the experiment reported, filters were used to eliminate the scattered excitation, and no attempt was made to monitor the individual fluorescence lines.

Finally, the relationship of ion pair absorption processes to the $Eu^{3+}$ terminated $Cr^{3+}$ fluorescence reported above by van der Ziel and Van Uitert should be mentioned. They have reported results explained by the emission of a photon corresponding to the difference in energy between simultaneous transitions in $Cr^{3+}$ and $Eu^{3+}$, but in opposite directions, the $Cr^{3+}$ losing energy, while the $Eu^{3+}$ ion goes from the ground state to an excited state. This could be viewed as an ion pair emission process, and serves to show the coupled nature of these trivalent ions in a suitable lattice.

4. Detailed Discussion of the Problem

The primary purpose of this investigation was to establish the occurrence of absorption of a single photon by a pair of dissimilar rare earth ions at low concentrations in $LaCl_3$. As has been mentioned, two ion absorptions have been reported previously only in high concentration samples.[1, 2]

The dopant ions should have energy levels such that the sums of pairs lie in a region free of single ion levels, so that the two ion processes will be distinguishable from the much stronger single ion processes. For these experiments, $Ho^{3+}$ and $Pr^{3+}$ were chosen as the dopants since the energy levels for both of these rare earths were known in $LaCl_3$ for low concentrations ($\sim$ 1%) and they met the above requirement.[4] In addition, $Nd^{3+}$ was known to be present as an impurity, in trace amounts. Pure $PrCl_3$ and $NdCl_3$ have $LaCl_3$ symmetry, while $HoCl_3$ has monoclinic symmetry (group $C_2$ about the $Ho^{3+}$ ion).

The single ion energy levels of $Ho^{3+}$ in $LaCl_3$ have been reported to high precision by Dieke and Pandey,[16] and those of $Pr^{3+}$ in $LaCl_3$ by Sarup and Crozier[33] and Dieke and Sarup.[34] $Nd^{3+}$ in $LaCl_3$ has been investigated by Carlson and Dieke[35, 36] and Varsanyi and Dieke.[37] Figure 1 shows the $Ho^{3+}$, $Pr^{3+}$, and $Nd^{3+}$

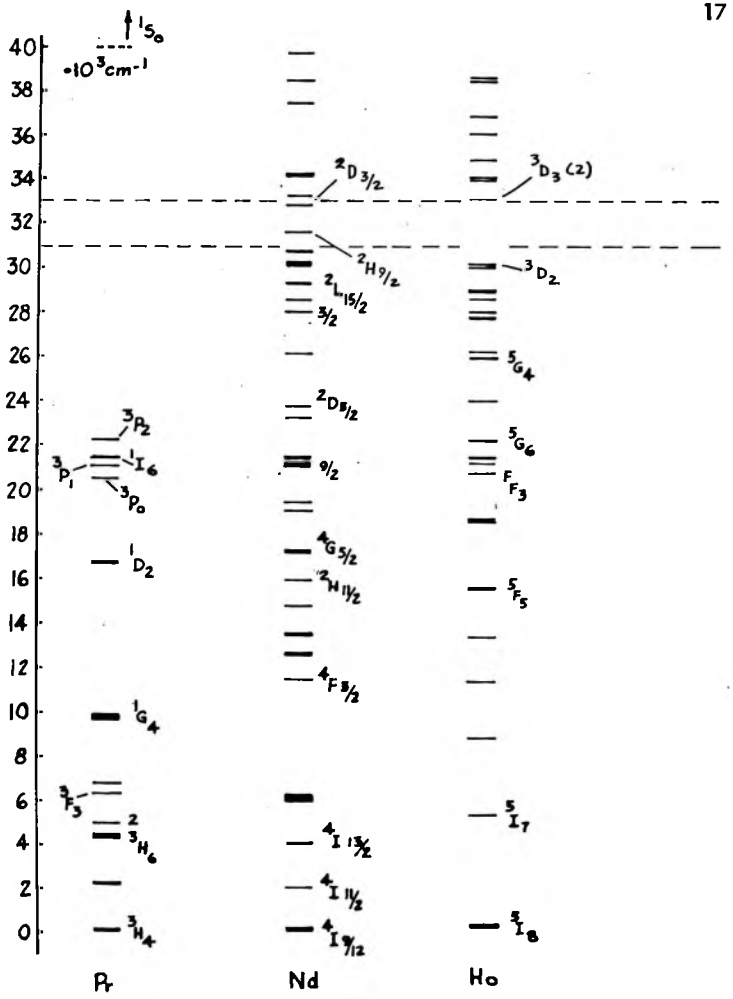


Figure 1. Energy levels of $Ho^{3+}$, $Pr^{3+}$, and $Nd^{3+}$ in $LaCl_3$ (from Reference 38).

energy level schemes in $LaCl_3$.[38]

For the rest of this discussion, it will be assumed that all ions are diluted in $LaCl_3$. The significant fact is that in $Pr^{3+}$, there are no single ion energy levels from the $^3P_2(2)$ at 22,247 $cm^{-1}$ to the $^1S_0(0)$ at approximately 48,800 $cm^{-1}$, while in $Ho^{3+}$ there is a gap between the $^3D_2$ level at 30,747 $cm^{-1}$ and the $^3D_3(2)$ level at 33,056 $cm^{-1}$. In $Nd^{3+}$ there is a gap between the $^4D_{3/2}$ level at approximately 32,800 $cm^{-1}$ and the $^2H_{9/2}$ level at approximately 31,500 $cm^{-1}$. The net gap between these two $Nd^{3+}$ levels is the smallest, being approximately 1300 $cm^{-1}$ wide.

It can be seen that there are three pair of Ho + Pr levels, two pair of Ho + Ho levels, and one pair of Pr + Pr levels whose sum energies fall in the above gap. In addition, in the same gap, there are Nd levels which combine with the Pr levels $^3P_2$, $^1I_6$, $^3P_1$, and $^3P_0$, and with eight Ho levels that decay to the $^5F_3$ or $^5F_5$ levels. These pair energy levels and their energy ranges (from Dieke[4]) are given in Table I below.

Table I. Ion pair absorption processes and their energy ranges near 32,000 $cm^{-1}$.

| Process | Range ($cm^{-1}$) |
|---|---|
| a) Ho + Pr processes | |
| 1. $Ho^{3+}(^5F_5) + Pr^{3+}(^1D_2)$ | 32,082 to 32,300 |
| 2. $Ho^{3+}(^5G_6) + Pr^{3+}(^1G_4)$ | 31,789 to 32,336 |
| 3. $Ho^{3+}(^5G_4) + Pr^{3+}(^3F_3)$ | 32,041 to 32,241 |
| b) Ho + Ho and Pr + Pr processes | |
| 4. $Ho^{3+}(^5F_3) + Ho^{3+}(^5I_5)$ | 31,776 to 31,889 |
| 5. $Ho^{3+}(^5G_5) + Ho^{3+}(^5I_6)$ | 32,555 to 32,661 |
| 6. $Pr^{3+}(^3P_2) + Pr^{3+}(^1G_4)$ | 31,940 to 32,174 |
| c) Pr + Nd processes | |
| 7. $Pr^{3+}(^3P_0) + Nd^{3+}(^4F_{3/2})$ | 31,899 to 31,929 |
| 8. $Pr^{3+}(^3P_1) + Nd^{3+}(^4F_{3/2})$ | 32,490 to 32,550 |
| 9. $Pr^{3+}(^1D_2) + Nd^{3+}(^2H_{11/2})$ | 32,538 to 32,741 |
| 10. $Pr^{3+}(^1I_6) + Nd^{3+}(^4F_{3/2})$ | 32,723 to 32,865 |

Table I. Ion pair absorption processes and their energy ranges near 32,000 $cm^{-1}$ (cont.).

| d) Ho + Nd processes | |
|---|---|
| Process | Range $cm^{-1}$ |
| 11. $Ho^{3+}\left({}^3H_5\right) + Nd^{3+}\left({}^4I_{13/2}\right)$ | 31,530 to 31,799 |
| 12. $Ho^{3+}\left({}^5G_2\right) + Nd^{3+}\left({}^4I_{13/2}\right)$ | 31,894 to 32,059 |
| 13. $Ho^{3+}\left({}^3K_7\right) + Nd^{3+}\left({}^4I_{15/2}\right)$ | 31,980 to 32,316 |
| 14. $Ho^{3+}\left({}^3H_6\right) + Nd^{3+}\left({}^4I_{13/2}\right)$ | 32,182 to 32,440 |
| 15. $Ho^{3+}\left({}^5F_2\right) + Nd^{3+}\left({}^4F_{3/2}\right)$ | 32,497 to 32,528 |
| 16. $Ho^{3+}\left({}^5F_5\right) + Nd^{3+}\left({}^4G_{5/2}\right)$ | 32,554 to 32,815 |
| 17. $Ho^{3+}\left({}^5G_3\right) + Nd^{3+}\left({}^4I_{13/2}\right)$ | 32,704 to 32,894 |
| 18. $Ho^{3+}\left({}^3K_8\right) + Nd^{3+}\left({}^4F_{3/2}\right)$ | 32,712 to 32,865 |

The above pair energy levels, as well as all single ion levels in the vicinity of 32,000 cm, are shown in Figure 2.

In addition, Porter and Edwards[39, 40] have shown that monochromatic excitation can produce broad band "continuum" fluorescence in alkali halides. The intensity of the "continuum" fluorescence is a very slowly varying function of the excitation wavelength, so that it should be possible to distinguish it from any process involving the direct excitation of a given level.

The decay schemes of the $Ho^{3+}$, $Pr^{3+}$ and $Nd^{3+}$ excited levels involved will be discussed next. The decay scheme for ions in the several $Ho^{3+}$ levels involved in the pair process with $Pr^{3+}$ is shown in Figure 3. Excitation of the $^5F_5$ level produces radiative transitions to the $^5I_7$ and the $^5I_8$ (ground) levels. The energies of these photons range from 10,280 to 10,800 $cm^{-1}$ and from 15,300 to 15,455 $cm^{-1}$ respectively.

The $^5G_6$ level decays by multiphonon emission to the $^5F_3$ level,[17] which decays in two ways; nonradiatively to the $^5F_5$ level by a pair process (which involves exciting an adjacent ion up from the ground level $^5I_8$ to the level $^5I_7$) and radiatively to the $^5I_7$ and $^5I_8$ levels (15,414 to 15,471 $cm^{-1}$ and 20,377 to 20,590 $cm^{-1}$

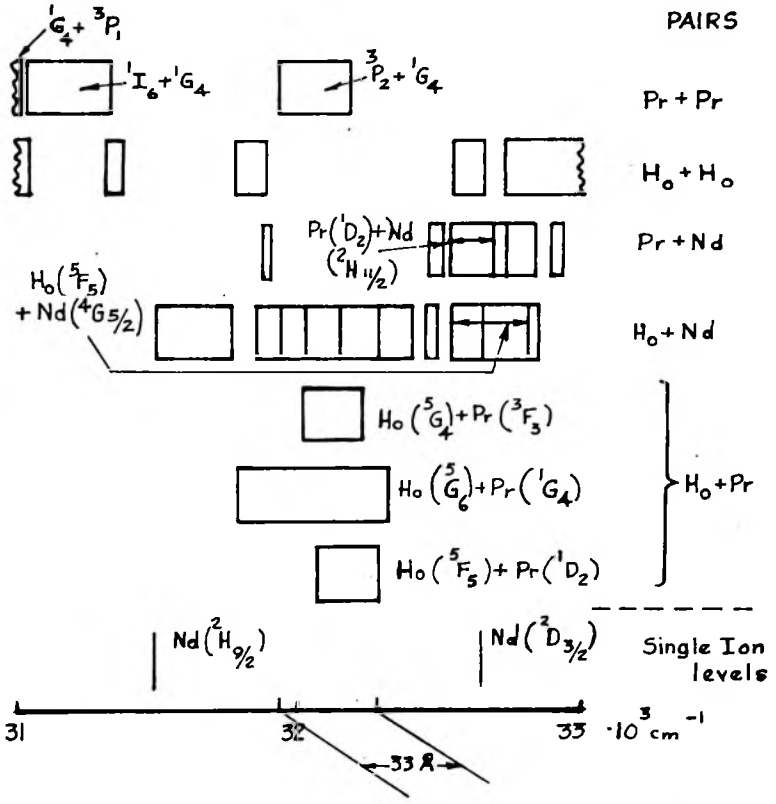


Figure 2. Single ion and pair energy levels near 32,000 $cm^{-1}$.

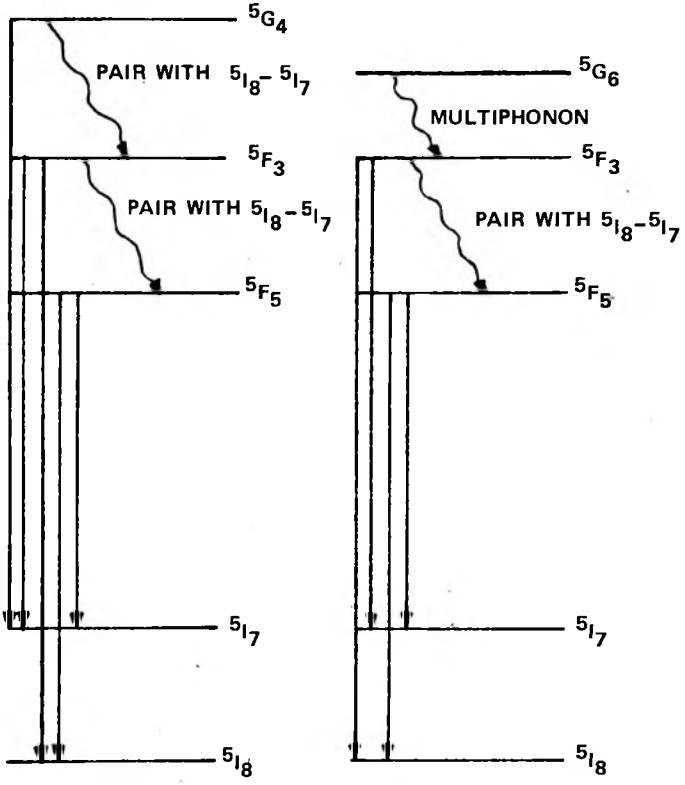


Figure 3. Decay scheme of $Ho^{3+}$ levels $^5G_4$, $^5G_6$, $^5F_3$, and $^5F_5$ in $LaCl_3$.

respectively). It should be noticed that the $^5F_3$ to $^5I_7$ radiation is in the same wavelength range as that from $^5F_5$ to $^5I_8$, as would be expected if ions in these levels were connected by a pair process. Thus, if ions were only excited to the $^5F_5$ level, the fluorescence spectrum in the vicinity of 15,400 $cm^{-1}$ would be different than if either ions were excited to the $^5G_6$ level alone and subsequently decayed to the $^5F_5$ level or if ions were excited to both the $^5G_6$ and the $^5F_5$ levels.

Ions at the $^5G_4$ level decay nonradiatively to the $^5F_3$ level by a pair process with $^5I_8$ to $^5I_7$, and also radiatively directly to $^5I_7$ (20,598 to 20,655 $cm^{-1}$ at 4.2°K, and 20,658 to 20,708 $cm^{-1}$ at 77°K). This radiative transition lies just to the short wavelength side of the transition $^5F_3$ to $^5I_8$. Once an ion reaches the $^5F_3$ level, the decay scheme would be similar to that with $^5G_6$ excitation.

Of the $Ho^{3+}$ levels involved in the Ho + Ho ion pair processes, the $^5F_3$ decay scheme has already been discussed. Ions excited to the level $^5G_5$ decay radiatively and by ion pair processes which do not involve the levels $^5F_3$ and $^5F_5$, and are not further discussed in this paper. Ions at the level $^5I_5$ decay radiatively to the $^5I_8$ level emitting photons of energy 11,109 to 11,209 $cm^{-1}$.

All of the $Ho^{3+}$ levels involved in the Ho + Nd ion pair processes decay in some manner to the $^5F_3$ level except for the $^5F_5$ level involved in process (16). With the exception of the $^5F_5$ level, the decay schemes of the $Ho^{3+}$ levels involved will not be discussed here, since the experimental results, given in Chapter III, gave evidence that ions were not excited to the $^5F_3$ level by excitation at approximately 32,000 $cm^{-1}$, and thus processes which might populate the $^5F_3$ level from above were evidently not operating.

The decay scheme of $Pr^{3+}$ in $LaCl_3$ is somewhat simpler than that of $Ho^{3+}$. If an ion is excited to the $^1D_2$ level, it can radiate to the $^3F_2$ level, the $^3H_6$ level, and the $^3H_4$ ground level. The radiation to the $^3F_2$ level has been observed by Sarup[41] to be extremely weak. The other two transitions range from 12,335 to 12,401 $cm^{-1}$ and from 16,333 to 16,534 $cm^{-1}$.[41] Radiation corresponding to transitions from ions at the $^1G_4$ and the $^3F_3$ levels to lower levels has not been reported in the literature, although Moos[42] indicates that both of the levels do fluoresce in $LaCl_3$. Ions excited to the levels $^1I_6$ and $^3P_1$ have been observed to undergo radiative transitions to lower levels,[41] but the radiation is very weak. Radiation is not observed from ions at the $^3P_2$ level. The primary means of

de-excitation is nonradiative decay by multiphonon emission to the $^3P_0$ level, and then by a combination of nonradiative decay to the $^1D_2$ level and by strong radiative transitions to lower levels.

The states of $Nd^{3+}$ in $LaCl_3$ that will be discussed here are those designated as the $^4G_{5/2}$, the $^2H_{11/2}$ and the $^4F_{3/2}$. Ions in the $^4G_{5/2}$ level are reported to decay to the $^4I_{9/2}$ (ground) and $^4I_{11/2}$ (first excited) levels, with fluorescence energies of 16,890 to 16,980 $cm^{-1}$ and from 15,036 to 15,125 $cm^{-1}$ respectively. These lines are strong but diffuse. Ions at the level $^2H_{11/2}$ are not reported to fluoresce strongly at 4.2°K. The transitions from $^2H_{11/2}$ to $^4I_{9/2}$ and $^4I_{11/2}$ range from 15,809 to 15,907 $cm^{-1}$ and from 13,848 to 13,987 $cm^{-1}$. These lines are extremely faint at 4.2°K, and are slightly stronger but very diffuse at 77°K. Ions at the $^4F_{3/2}$ level undergo radiative transitions to the $^4I_{9/2}$ level with a range of 11,174 to 11,389 $cm^{-1}$. Only one line, at 11,301 $cm^{-1}$, is reported to be strong at 4.2°K.[43]

5. Experimental Approach

The first experiment performed on the doped $LaCl_3$ crystals was the search for fluorescence excited in the 1%Ho, 1%Pr and 1%Ho + 1%Pr samples at 4.2°K with approximately 32,000 $cm^{-1}$

(3100 Å) excitation. The $Pr^{3+}$ levels monitored were the $^1D_2$, the $^3P_0$, and the $^3P_1$, those in $Ho^{3+}$ were the $^5F_5$, $^5F_3$, and the $^5G_4$, and in $Nd^{3+}$, the $^4G_{5/2}$, as these were reported to fluoresce in the single doped crystals.[16, 41, 43] Several other excitation energies were used to help in establishing the origin of the observed fluorescence.

Next, an excitation spectrum was made for each of the major fluorescence transitions in both the single and double doped crystals at 4.2°K. In this process, the fluorescence monitoring spectrometer was set on the fluorescence line, and the excitation monochromator was scanned in order to see if there was a peak in the fluorescence at the excitation wavelength corresponding to the pair absorption energy. In making this set of measurements, it was found that the variation of the "continuum" radiation due to the variation of the intensity of the excitation source with wavelength was sufficiently large to hide the small excitation peaks of the pair absorption process. It was thus necessary to make normalized excitation spectra, in which the fluorescence output is compensated for the spectral intensity variations of the excitation source.

The peaks in the normalized excitation spectrum at the proper pair absorption energy are evidence that the pair absorption process is indeed operating in the crystal under investigation. However, the resolution was not high enough to establish which levels in the Stark manifolds created by the crystal field splitting were involved in the pair process. This information would be extremely useful to establish some sort of selection rules for ion pair absorption, if, indeed, there are any.

In order to obtain this information, it is necessary to get a high resolution absorption spectrum on the double doped crystal. Dieke and Dorman[2] have reported two ion absorptions in 100% $PrCl_3$, and on the basis of these experiments, it was expected that the two ion absorptions would be many magnitudes weaker than that for single ions. In addition, it was felt that the absorption measurements could give valuable information about the impurities present in the samples and possibly some idea of the strength of the Ho + Pr and Pr + Pr pair process relative to those processes due to the impurities present. Photographic absorption measurements were made on the double doped and single doped crystals at $4.2^{\circ}K$, with excitation covering the range around 32,000 $cm^{-1}$ as well as towards longer wavelengths

(where the Pr + Pr absorption levels had been observed in 100% $PrCl_3$ by Dieke and Dorman).

# CHAPTER II

## EXPERIMENTAL DETAILS

### 1. Samples and Cooling

All samples used were made by doping anhydrous 99.999% pure $LaCl_3$ with small amounts of comparable purity $PrCl_3$, or 99.9% pure $HoCl_3$, or both. These high purity anhydrous chlorides were supplied by Lindsay Division, American Potash and Chemical Corporation. The samples were grown by J. F. Porter, Jr., by the method of Hutchisson and Wong.[44] The 1%Ho: 1%Pr: $LaCl_3$ samples were transparent polycrystalline prisms approximately 4 by 4 by 11 mm., sealed in a quartz tube which was backfilled with one half atmosphere of helium to assure thermal contact with the bath. The 1% Pr: $LaCl_3$ sample was a single crystal of approximately the same size, and mounted in the same manner. The 1%Ho: $LaCl_3$ sample was in powdered crystal form, and sealed and mounted the same way. A polycrystalline sample of 1%Ho: 1%Nd: $LaCl_3$ was also used in the absorption study. The primary impurities in the Ho and Pr doped crystals have been identified as $Pr^{3+}$ and $Nd^{3+}$ by Porter.[17]

The encapsulated samples were immersed in liquid helium in a 1.3 liter quartz window double dewar, which could retain helium for up to 6 hours, depending on the intensity of the incident radiation. The dewar is of conventional design, with a gold plated copper heat shield at liquid nitrogen temperature completely encasing the quartz inner tip, except for a small aperture to allow absorption and fluorescence measurements. The bubbles formed in the liquid helium during the experiment did not cause the sample to move noticeably, but did scatter a small amount of light.

2. Excitation Sources

a. Broad Band Source

For absorption measurements, a broad band ultraviolet source was needed, and a GE AH-6, 1 kw high pressure mercury arc lamp was chosen. This lamp was operated within a water-cooled quartz housing made by George W. Gates and Co. and was powered by a 1200 V transformer. In most of the absorption experiments, a 10 cm water cell with quartz windows was used to absorb the infrared radiation and minimize the heating of the sample and liquid helium.

b. Monochromatic Excitation

The GE AH-6 lamp was again used for monochromatic excitation, but in conjunction with a Bausch and Lomb 500 mm monochromator with a quartz condenser system. The grating used had 600 lines/mm, blazed at 5000 Å, with a dispersion of 33 Å/mm. The slit width used was 1 mm. The wavelength drum of the monochromator was driven with a synchronous Insco gear motor and a PIC Corporation toothed belt and pulleys.[17] Drive speeds of 40 and 100 Å/min were used. No filters were used in the excitation wavelength range of from 2600 to 4000 Å.

The primary difficulty associated with using the AH-6 lamp is that while it has an output which is rich in ultraviolet, it also contains strong pressure broadened emission lines which make an excitation spectrum taken with this source hard to interpret unless normalized to constant excitation intensity. Figure 4 shows the spectral distribution of energy from the AH-6 mercury lamp-monochromator combination, scanned at 100 Å/min with 1 mm entrance and exit slits. The short zero trace at the end of the spectrum was taken with the lamp blocked off, to show the negligible effect of room light. The output beam was chopped at 14 hz by a Princeton Applied Research

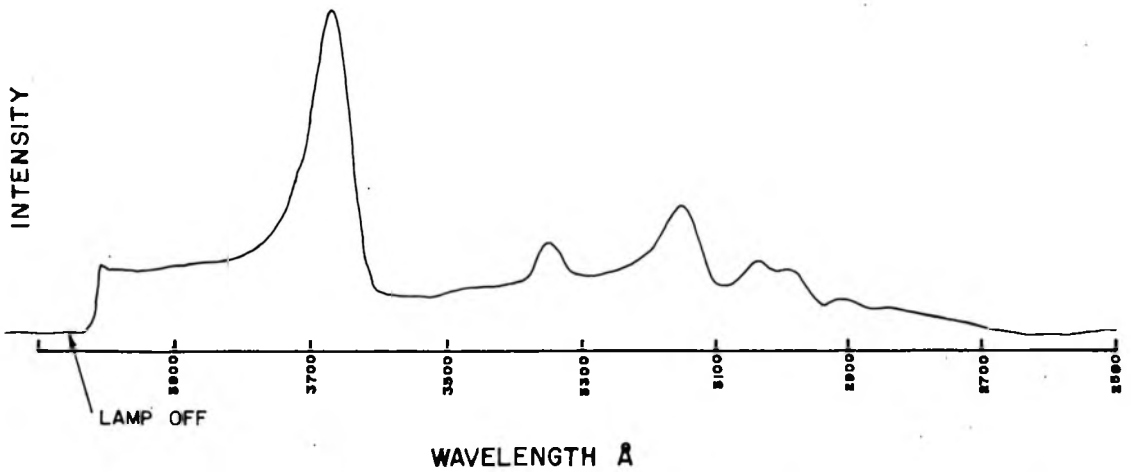


Figure 4. Spectral distribution of GE AH-6 mercury lamp and B and L 500 mm monochromator.

(PAR) BZ-1 chopper, and focussed by a quartz lens on a Charles Reeder RDE-1 thermocouple with a quartz window. The thermocouple output was detected on a PAR HR-8 lock-in amplifier with a Type B preamplifier (100:1 transformer). Figure 5 shows the optical and electrical layout.

3. Fluorescence Equipment

The fluorescence measurements were made on the doped $LaCl_3$ samples at 4.2°K with the monochromatic source previously mentioned and the 0.3 meter McPherson scanning monochromator using a 1200 line/mm grating blazed at 5000 Å (26.5 Å/mm dispersion). This is a very fast (f/5.3) monochromator, and thus is suitable for detecting the extremely weak fluorescence produced in the two ion process. Slit widths generally used were 100 or 200 $\mu$, and scan speeds of 5 or 10 Å/min, while the excitation monochromator was held fixed. These large slits, and subsequent low resolution, were made necessary by the weakness of the fluorescence. The detector was an EMI 9558Q photomultiplier (S-20 response), powered by a Fluke high voltage power supply. Fluorescence measurements at wavelengths longer than the infrared cut off of the photomultiplier

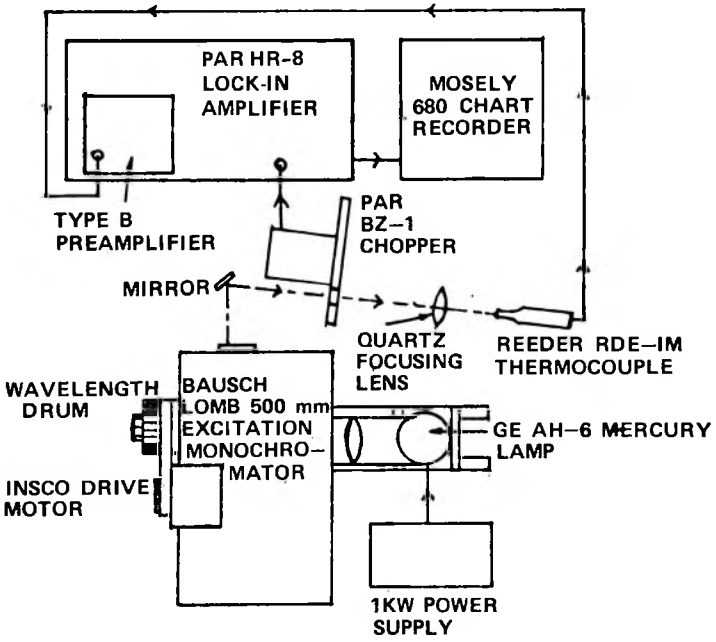


Figure 5. Optical and electrical layout for spectral distribution measurement.

($\gtrsim$ 7500 Å) were made with a Kodak Ektron type Q-2 PbS detector, cooled to dry ice-acetone temperature (-78° C). A White Instruments Type 256 transistor active filter tuned to 14 hz was used in conjunction with a cathode follower to amplify the signal from the PbS cell. The circuit diagram is shown in Figure 6. All first surface aluminum coated reflective optics were used in the system except for the filters placed before the entrance of the detector monochromator to filter out the excitation. The filters used were of two types, Corning polished glass filters (designated by number, e.g., 0-52), and Optics Technology Vari-Pass dialectric coated interference filters (designated by band pass, e.g., > 4500 Å). Outside of the region of transmittance, the transmission was generally $\lesssim$ 0.1%.

The fluorescence was mechanically chopped before entering the monochromator, and the output of the photomultiplier was detected by a PAR HR-8 lock-in amplifier with a type A preamplifier, finally driving a Mosely model 680 strip chart recorder. A typical time constant used on the lock-in amplifier was 1 sec/12 db, with a slower time constant and scan being required by a higher noise level. Figure 7 shows the optical and electrical layout for this experiment.

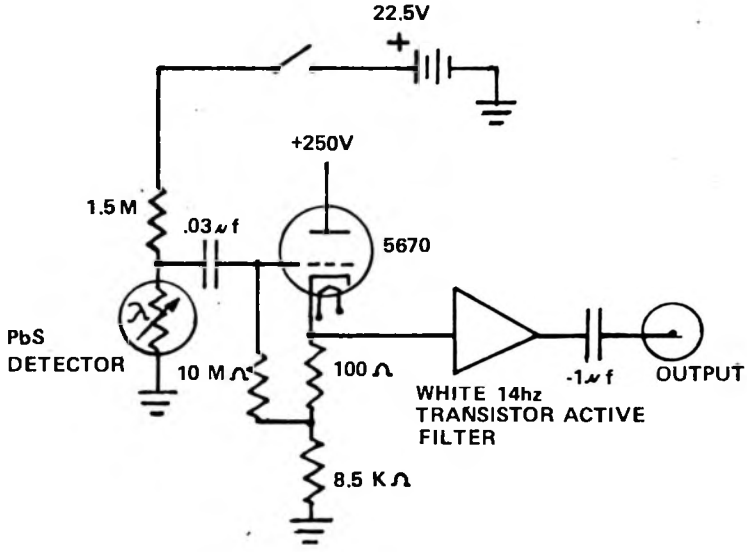


Figure 6. Cathode follower circuit and tuned active filter used with PbS cell.

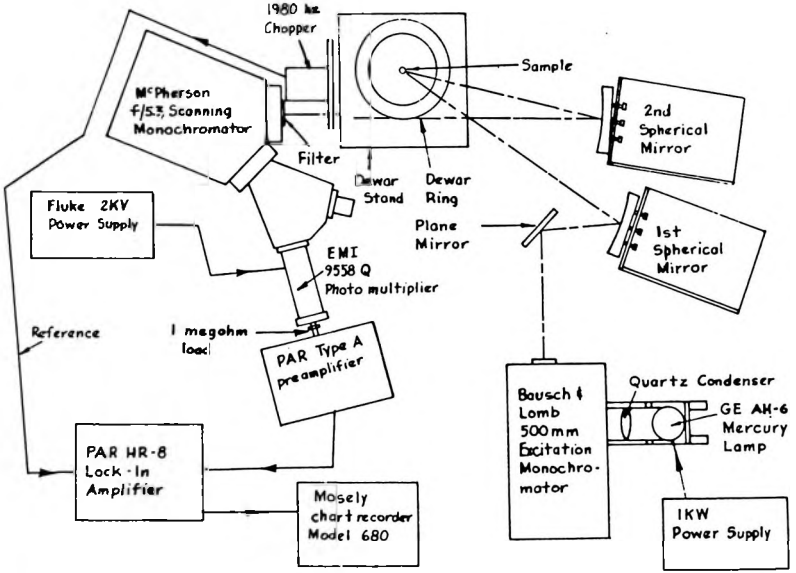


Figure 7. Optical and electrical layout for fluorescence measurements.

4. Preliminary Excitation Equipment

The preliminary excitation experiments were carried out on the same equipment previously described for the fluorescence measurements, but in this case, the excitation monochromator was scanned rather than the fluorescence monochromator. The fluorescence signal was peaked up by setting the excitation monochromator so as to excite a single ion level which was known to produce the desired fluorescence and then adjusting the fluorescence monochromator for the maximum signal.

5. 1980 hz Chopper

In order to reduce the photomultiplier noise, which is inversely proportional to the frequency, it was decided to go to a higher chopping frequency. The highest frequency that the PAR BZ-1 chopper can achieve is approximately 600 hz, and it is not particularly stable at this frequency, due to slippage in the rubber belt drive. It was decided to build a direct drive chopper to eliminate these problems. A 3600 rpm Bodine hysteresis synchronous motor type KYC-26-704 was chosen, and a 33 blade chopper wheel was fabricated out of 0.813 mm (0.032 in.) aluminum. It was necessary to keep the diameter of this

blade to 12 cm in order to minimize the moment of inertia, as well as to provide clearance for the photomultiplier housing. The motor was able to synchronize the new blade within less than a second after turn on, as determined by observation with a strobe lamp. The reference pulse circuit is formed by a Texas Instrument H-11 photodiode and a 1.4 v mercury battery, all driven by a TS-327 bulb operating at 20 v for increased bulb life. The electrical schematic is shown in Figure 8. Figure 9 shows the chopper blade and the special pot chuck in which it was made, and Figure 10 shows the completed chopper. All the mechanical parts of the chopper, as well as the pot chuck, were made by Mr. John Medlin and Mr. Lloyd Sharpe of the University of Alabama Research Institute. Upon assembly, the chopper proved stable to within $\pm 0.2$ hz at 1980 hz, for short periods (1 hour), and to line frequency accuracy for long periods. When using the photomultiplier at this chopping frequency, it was necessary to mount the preamplifier as close to the photomultiplier as possible, in order to minimize signal loss. This was done with a PAR remote preamplifier adapter.

6. Absorption Equipment

The absorption plates were taken on a Bausch and Lomb 2.0 meter

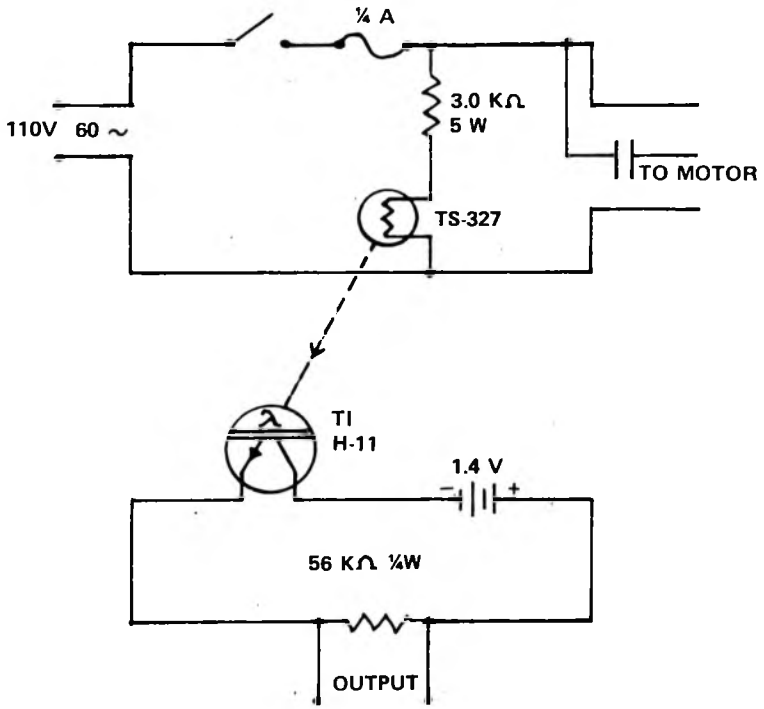


Figure 8. 1980 hz chopper schematic.

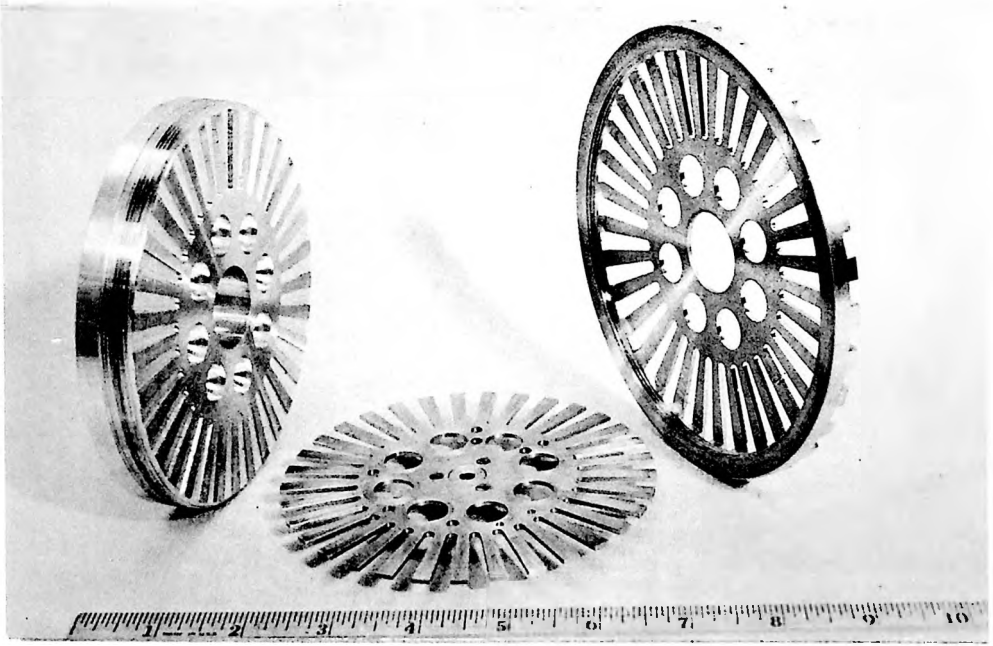

Figure 9. 1980 hz chopper blade and pot chuck.

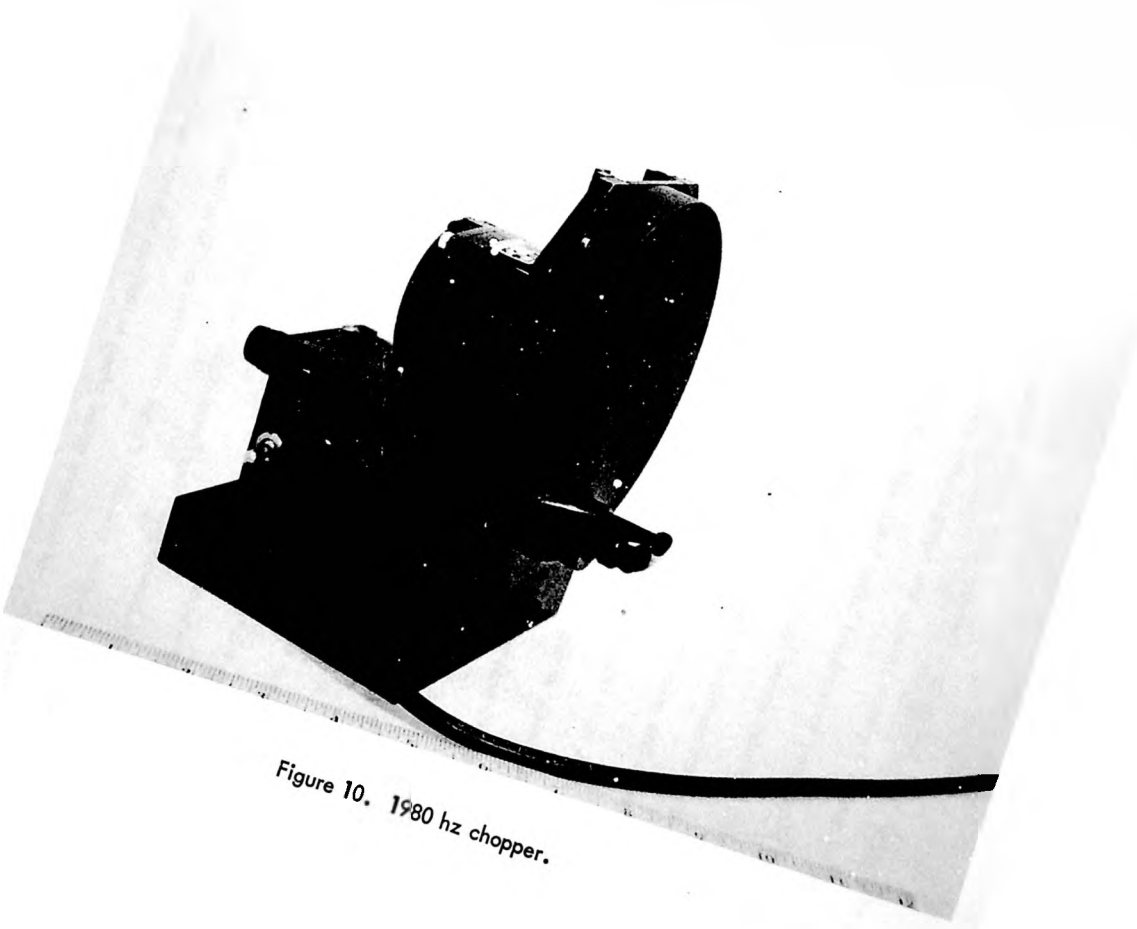

Figure 10. 1980 hz chopper.

spectrograph with a 1200 line/mm grating and 10 $\mu$ slits. The plate factor for this spectrograph was approximately 4 Å/mm in the range of 3000 to 4000 Å. The AH-6 broad band source previously described was used in conjunction with an optical bench mounted dewar stand and all quartz optics. The dewar stand is designed to be conveniently adjustable so as to accommodate different samples and dewars, and is shown in Figure 11. Kodak 103-0 plates were used from 2900 to 5000 Å, and 103-F plates from 5000 to 7000 Å. All plates were stored under refrigeration before exposure and processed according to standard Kodak procedures.

7. Normalized Excitation Equipment

The monochromatic source previously described was used in conjunction with the McPherson 0.3m monochromator to make normalized excitation spectra. This technique was necessary because the variation of the intensity of the "continuum" radiation caused by the spectral variation of the excitation lamp's intensity with wavelength was greater than the excitation peaks being searched for. A microscope slide was used to reflect a fraction of the beam through a quartz lens and 14 cps chopper, into the Reeder thermocouple.

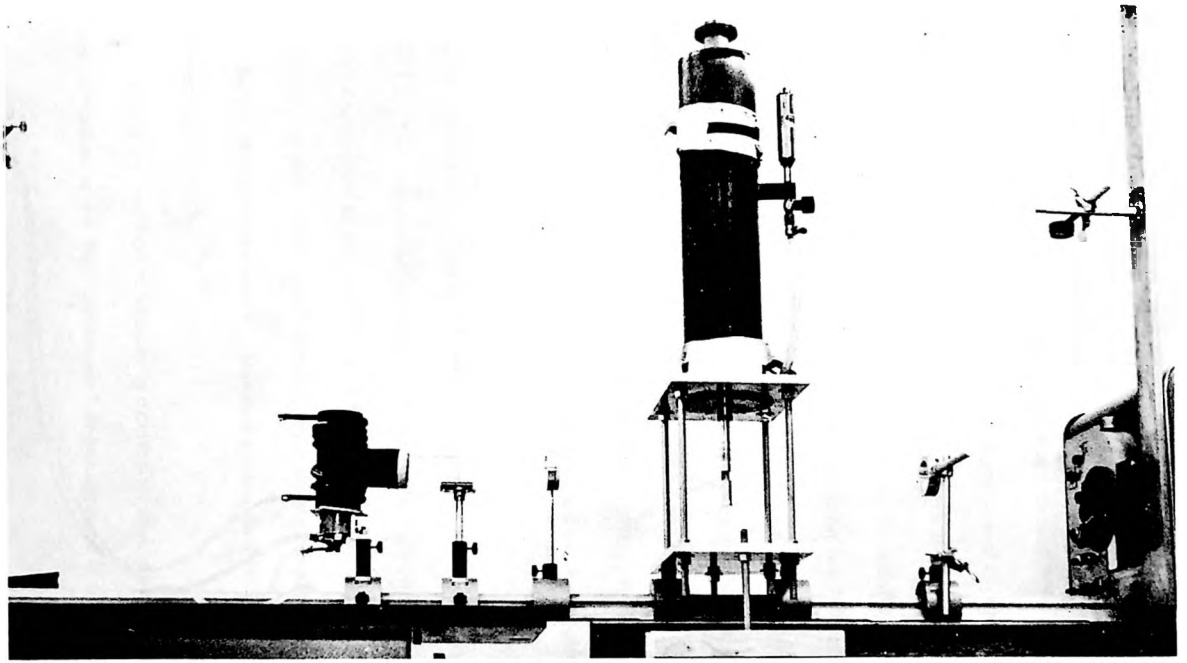

Figure 11. Optical bench and dewar stand used for absorption measurements.

This signal was detected on the PAR HR-8 lock-in amplifier with the type B preamplifier. The fluorescence was focussed by a spherical first surface mirror through the 1980 hz chopper and an appropriate filter into the McPherson monochromator, where it was detected by the photomultiplier. This signal was processed by another PAR HR-8 with a type A preamplifier. Both signals are then fed into a Mosely model 7100 B two pen recorder and also to a Pace TR-10 analog computer, programmed to divide the fluorescence output by the excitation output. The output of the analog computer is fed to a second Mosely recorder, model 680. The fluorescence signal, the excitation signal, and the fluorescence signal divided by the excitation signal are all thus displayed. The optical layout and electrical block diagram is shown in Figure 12, and the computer schematic in Figure 13. The theory and details of the circuit are given in Appendix A. Proper operation of this technique is based on the assumption that the intensity of the "continuum" radiation is a slowly varying function of the excitation wavelength. This was established for $LaCl_3$ by Porter and Edwards.[39, 40]

The above method of obtaining excitation spectra will work in any situation where the "continuum" or background is a slowly

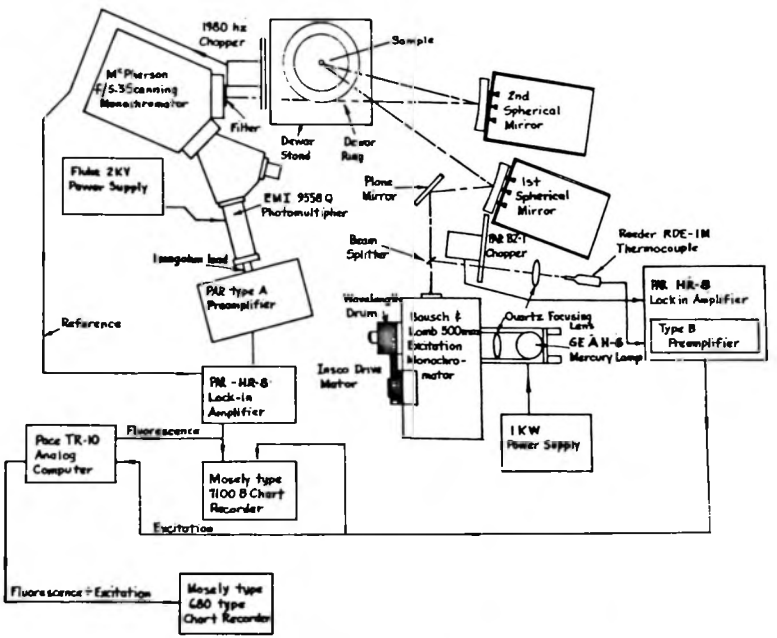


Figure 12. Optical and electrical layout for normalized excitation measurements.

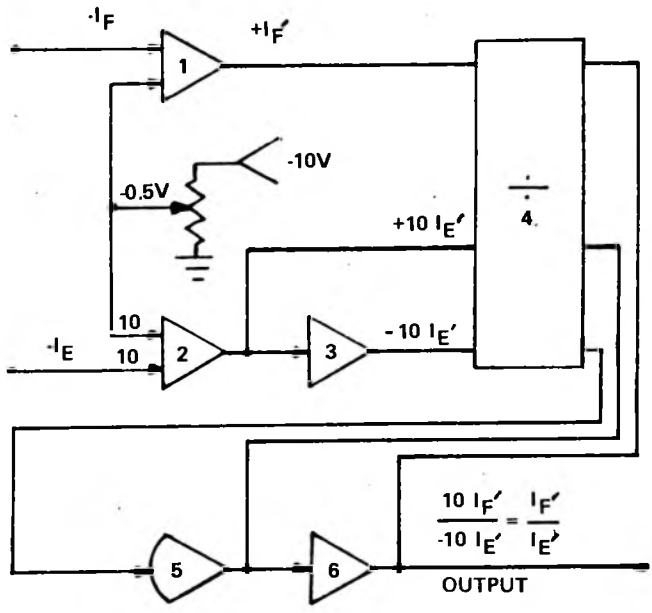


Figure 13. Analog computer schematic for normalized excitation measurements.

varying function of wavelength, and, in addition, will work with any type of spectrometer, the only restriction being that the signals be of such level that they can be accurately processed electronically. In essence, the effect is that of having a source that is "flat" in output as a function of wavelength (providing that the detector is flat in response), exactly as if one had employed an intensity operated slit servo system, but with the advantage that the variable resolution attendant with a variable slit is eliminated. In this way, one is able to probe for weak pair processes in the vicinity of any excitation line that is not so strong as to overload the analog computer.

8. Calibration

The wavelength scales of all spectrometers were calibrated with an Ultra Violet Products, Inc. low pressure mercury discharge lamp. The 500 mm Bausch and Lomb excitation monochromator had a wavelength drum marked in 10Å increments, and was accurate to within +10 Å at 1 mm slit width. The scale was repeatable to within ±5 Å at 1 mm slits. The 0.3 meter McPherson monochromator had a Veeder-Root wavelength counter which read to 1 Å, and could be adjusted to be accurate to within at least 1 Å. In most cases, instead

of adjusting the counter, it was sufficient to simply note the counter reading at a known calibration wavelength and given slit setting. All photographic plates taken on the 2.0 meter Bausch and Lomb spectrograph were calibrated by alternating the absorption spectra with mercury discharge lamp emission spectra, in such a manner that the spectra overlapped slightly.

The lock-in amplifiers are provided with internal calibration standards, which were used to check the gain of the amplifiers. Since comparisons were only made between intensity ratios taken on one run versus ratios taken on another run, it was sufficient to verify that the gain did not change during a given run. In fact, the gain was stable during the entire series of experiments, provided no components (such as a preamplifier) were changed. All voltages on the analog computer were read by balancing against an internal standard, accurate to within $\pm 3\%$. All spectrometers, monochromators, and chart recorders were driven by synchronous motors, so line frequency accuracy can be expected for the constancy of drive speeds. Due to the use of voltage stabilizers, variations in line voltage had little or no effect upon the results.

# CHAPTER III

# EXPERIMENTAL RESULTS

## 1. Introduction

This chapter presents the experimental results, cited without discussion or analysis except where essential to provide continuity. Preliminary results have been reported by Porter and Blatt.[45] The analysis of the experimental results and conclusions drawn from them are presented in Chapter IV, and the conclusions are again presented in a condensed form in Chapter V. In this chapter and the chapters that follow, it will be understood that the crystal matrix used is anhydrous $LaCl_3$, with the various rare earths present as dilute dopants or impurities. Thus, when a given energy level of a rare earth ion is referred to, it is assumed that the ion is diluted in $LaCl_3$.

## 2. Noise and Background

The groups of fluorescence lines obtained are described in this chapter in terms of relative strengths (peak height) of the lines to one prominent line, usually the largest. These strengths are given with a

stated background level, and, sometimes with a stated noise level. The background level represents the sum of the "continuum" fluorescence and scattered light in the filter band pass, and is measured from the zero signal level at the bottom of the recorder paper. The noise level is the peak-to-peak height of the high frequency component of the fluorescence, and includes the dark current from the photomultiplier and random high frequency noise in the load resistor and amplifier. The line strengths are all measured from the average "continuum" or background level adjacent to the given fluorescence line. If no noise level is given, it may be assumed that the high frequency component was below 0.01 times the height of the reference line for a given group of fluorescence lines.

3. Fluorescence Measurements

a. 1%Ho: $LaCl_3$ Powdered Sample at 4.2°K

The 1%$Ho^{3+}$ doped sample was pumped with approximately 32,000 $cm^{-1}$ (3100 Å) excitation, and fluorescence lines were observed at approximately 6454, 6467, 6476, 6483, 6492, and 6513 Å, with strengths relative to the 6492 Å line of 0.32, 0.55, 0.49, 0.82, 1.0, and 0.47. The background level was approximately 0.24 and the

noise was 0.02 on the same scale. In Chapter IV, these lines will be assigned to the transitions $^5F_5 - {}^5I_8$. No other fluorescence lines attributable to $Ho^{3+}$ transitions greater than 1.2 times the background level were observed in the region from 6460 to 6520 Å and from 4860 to 4910 Å. At the same excitation, extremely weak fluorescence was observed at approximately 5932 and 6635 Å. The first transition was assigned to $Nd^{3+}\left({}^4G_{5/2} - {}^4I_{9/2}\right)$ and the second to $Nd^{3+}\left({}^4G_{5/2} - {}^4I_{11/2}\right)$ according to the results of Carlson.[43] The fluorescence observed is shown in Figures 14 and 15 and Table II.

The same sample was then excited at 4860 Å, which corresponds to direct excitation of single $Ho^{3+}$ ions to the $^5F_3$ level. The six $Ho^{3+}$ fluorescence lines reported above were observed, but in strengths relative to the 6492 Å line of 0.28, 0.56, 1.05, 1.14, 1.0, and 0.23, with a background level of 0.09. Based on the work of Dieke and Pandey,[16] these lines were attributed to $^5F_3 - {}^5I_7$ and $^5F_5 - {}^5I_8$ transitions. This fluorescence is shown in Figure 15 and Table II.

The sample was next pumped with 3880 Å radiation, exciting the ions to the $^5G_4$ level. Fluorescence lines were observed at approximately 4841 and 4853 Å with intensitites of 4.6 and 2.5,

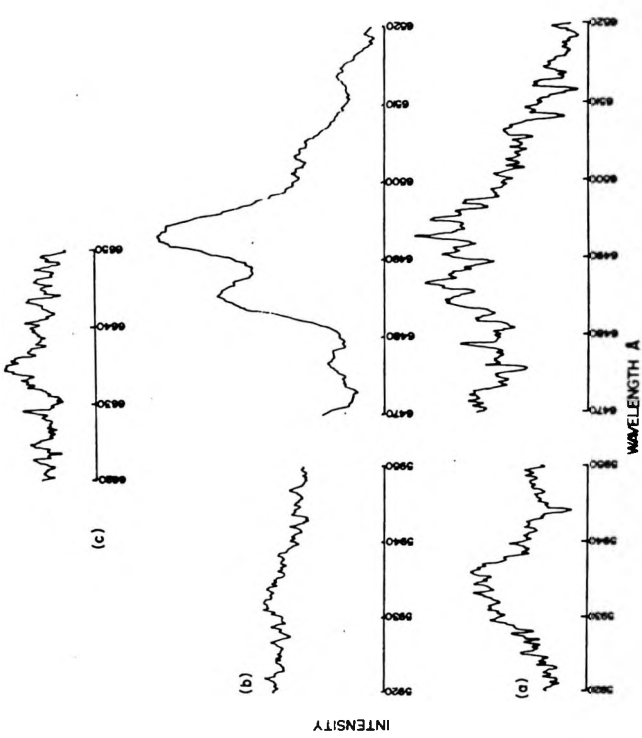


Figure 14. Fluorescence observed at 4.2°K under 32,000 $cm^{-1}$ excitation in (a) Ho:Nd:$LaCl_3$ from 5920 to 6520 Å, (b) Ho:$LaCl_3$ from 5920 to 6520 Å, (c) Ho:$LaCl_3$ from 6620 to 6650 A.

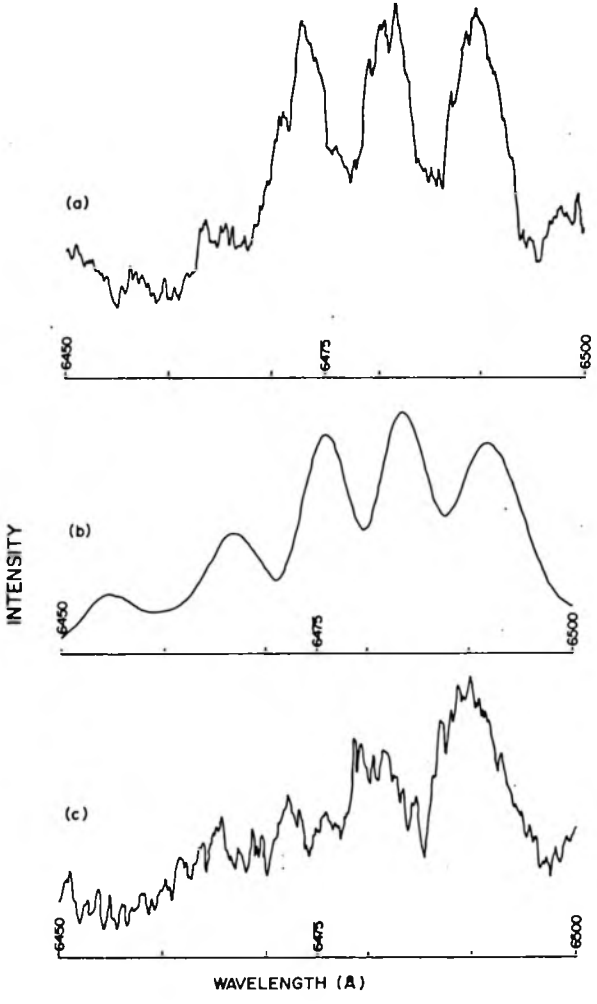


Figure 15. Fluorescence observed at 4.2°K from 6450 to 6500 Å in (a) Ho:Pr:$LaCl_3$ under 32,000 $cm^{-1}$ excitation, (b) Ho:$LaCl_3$ under 20,576 $cm^{-1}$ ($^5F_3$) excitation, (c) Ho:$LaCl_3$ under 32,000 $cm^{-1}$ excitation.

Table II. Relative intensities of $Ho^{3+}$ fluorescence lines in the 6454 to 6520 Å group at 4.2°K.

| Wavelength Å | Relative Intensity | | |
|---|---|---|---|
| | Ho: $LaCl_3$ 32,000 $cm^{-1}$ Excitation | Ho: $LaCl_3$ $^5F_3$ Excitation | Ho: Pr: $LaCl_3$ 32,000 $cm^{-1}$ Excitation |
| 6454 | 0.32 | 0.28 | 0.08 |
| 6467 | 0.55 | 0.56 | 0.22 |
| 6476 | 0.49 | 1.05 | 0.78 |
| 6483 | 0.82 | 1.14 | 0.92 |
| 6492 | 1.0 | 1.0 | 1.0 |
| 6513 | 0.47 | 0.23 | -- |
| Background | 0.24 | 0.09 | 0.34 |
| Noise | 0.02 | -- | 0.16 to 0.32 |

identified as corresponding to the transition $^5G_4 - {}^5I_7$, and at 4862, 4871, 4877, 4891, and 4906 Å with intensitites of 0.17, 0.9, 1.0, 0.27, and 0.49, which were assigned to the transition $^5F_3 - {}^5I_8$. The intensities are relative to the 4877 Å line, with the background level being 0.1 on the same scale. These fluorescence lines are shown in Figure 16 and Table III.

Finally, the sample was pumped with 4515 Å radiation, which corresponds to a direct excitation of ions to the $^5G_6$ level. The lines assigned to the transition $^5F_3 - {}^5I_8$ were again observed at 4853, 4862, 4871, 4877, 4891, and 4906 Å, with relative intensities of 0.07, 0.12, 0.91, 1.0, 0.30, and 0.54, with a background level of 0.01. These lines are also shown in Figure 16 and Table III.

b. 1%Pr: $LaCl_3$ Single Crystal Sample at 4.2°K

The 1%$Pr^{3+}$ doped sample was pumped at the $^3P_2$ energy level (4480 Å), and fluorescence was observed at approximately 6023, 6154, 6179, 6192, and 6440 Å, with relative signal strengths of 0.06, 0.33, 0.8, 0.06, and 1.0, with a background level of 0.02. Following Sarup,[41] these lines were assigned to the $Pr^{3+}$ transitions $^1D_2 - {}^3H_4$, $^3P_0 - {}^3H_6$ (3 lines), and $^3P_0 - {}^3F_2$. Figure 17 shows these fluorescence lines. Table IV gives the signal strengths relative

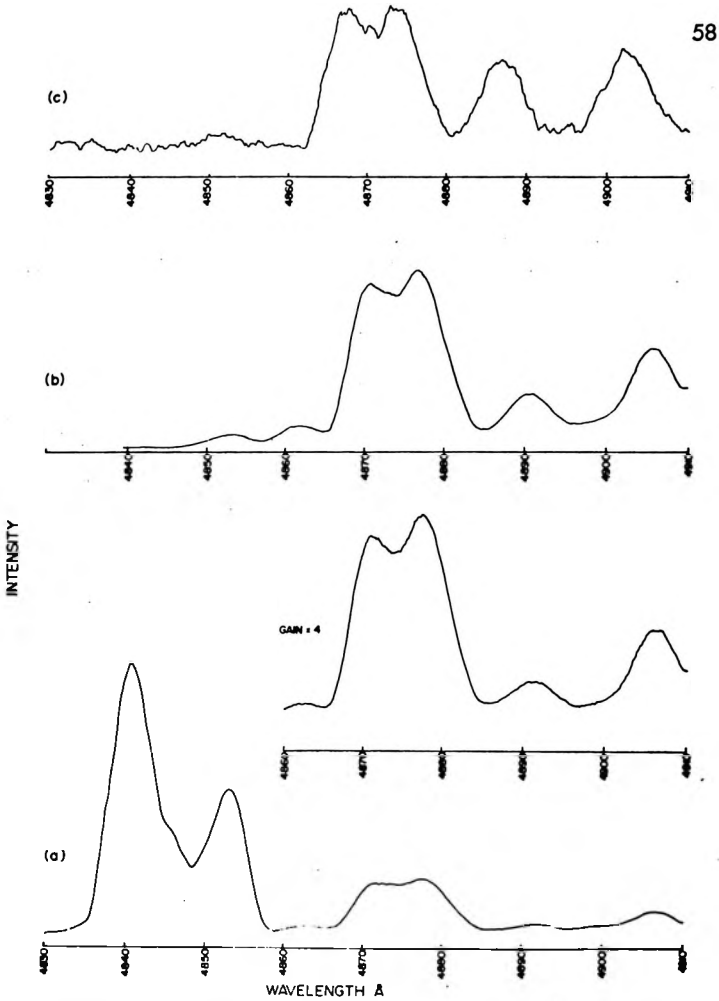


Figure 16. Fluorescence observed at 4.2°K from 4830 to 4910 Å in (a) Ho:$LaCl_3$ under 25,775 $cm^{-1}$ ($^5G_4$) excitation, (b) Ho:$LaCl_3$ under 22,148 $cm^{-1}$ ($^5G_6$) excitation, (c) Ho:Pr:$LaCl_3$ under 32,000 $cm^{-1}$ excitation.

Table III. Relative intensities of $Ho^{3+}$ fluorescence lines in the 4841 to 4906 Å group at 4.2°K.

| Wavelength Å | Relative Intensity | | |
|---|---|---|---|
| | Ho: $LaCl_3$ $^5G_4$ Excitation | Ho: $LaCl_3$ $^5G_6$ Excitation | Ho: Pr: $LaCl_3$ 32,000 $cm^{-1}$ Excitation |
| 4841 | 4.6 | -- | -- |
| 4853 | 2.5 | 0.07 | -- |
| 4856 | -- | -- | 0.12 |
| 4862 | 0.17 | 0.12 | -- |
| 4871 | 0.9 | 0.91 | 0.97 |
| 4877 | 1.0 | 1.0 | 1.0 |
| 4891 | 0.27 | 0.30 | 0.62 |
| 4906 | 0.49 | 0.54 | 0.71 |
| Background | 0.1 | 0.01 | 0.23 |
| Noise | -- | -- | 0.05 |

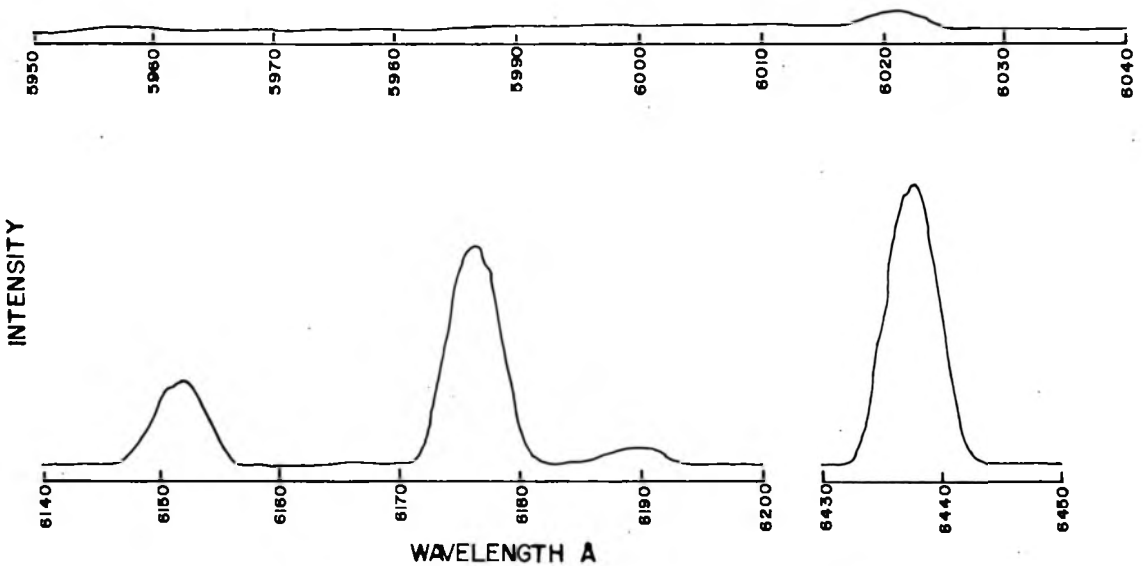


Figure 17. Fluorescence from $Pr:LaCl_3$ at 4.2°K under 22,252 $cm^{-1}$ ($^3P_2$) excitation.

Table IV. Relative intensities of $Pr^{3+}$ fluorescence lines in the 6023 to 6440 Å group at 4.2°K.

| Wavelength Å | Relative Intensities | | |
|---|---|---|---|
| | Pr: $LaCl_3$ $^3P_2$ Excitation | Pr: $LaCl_3$ 32,000 $cm^{-1}$ Excitation (Typical) | Ho: Pr: $LaCl_3$ 32,000 $cm^{-1}$ Excitation |
| 6023 | 1.0 | 1.0 | 1.0 |
| 6154 | 5.5 | 0.32 | 0.3 |
| 6179 | 13.4 | 0.48 | 0.45 |
| 6192 | 1.0 | -- | -- |
| 6440 | 16.7 | 0.64 | 0.14 |
| Background | 0.02 | 0.51 to 0.89 | 0.48 |
| Noise | -- | 0.09 | 0.33 |

to the 6023 Å line.

The sample was pumped with approximately 32,000 $cm^{-1}$ excitation and fluorescence was observed at approximately 6011, 6023, 6154, 6179, and 6440 Å. The first two lines were attributed to the $Pr^{3+}$ transition $^1D_2 - {}^3H_4$, the second two to $^3P_0 - {}^3H_6$, and the last one to $^3P_0 - {}^3F_2$. The ratio of the strength of the $^1D_2$ fluorescence to that of the $^3P_0$ fluorescence was found to vary widely, according to the length of time the sample was immersed in the liquid helium in the dewar. Shortly after immersion, the ratio of the largest signal (above background)of the $^1D_2$ fluorescence group (6023 Å) to that from the $^3P_0$ level (6440 Å) was about 0.3; after several hours in the dewar, the ratio rose to a maximum of 2.77. The ratio of the 6179 Å and the 6144 Å lines to the 6440 Å line was fairly constant at approximately 0.7 and 0.4 respectively. The 6013 Å line had a fairly constant ratio of about 0.3 to the 6023 Å line. The average strengths of all the lines for long and short immersion times are shown relative to the 6023 Å line below in Table V.

Table V. Effect of immersion time on relative intensities of fluorescence lines in 1%Pr: $LaCl_3$ under 32,000 $cm^{-1}$ excitation.

| Line (Å) | 6113 | 6023 | 6154 | 6179 | 6440 |
|---|---|---|---|---|---|
| Intensity (short immersion) | 0.3 | 1.0 | 1.33 | 2.5 | 3.5 |
| Intensity (long immersion) | 0.3 | 1.0 | 0.2 | 0.37 | 0.52 |

In the period between the measurements, the dewar containing the sample was not irradiated, showing that the effect was not due to radiative heating (greater than room temperature radiation) or bleaching. An example of this fluorescence is shown in Figure 18 and Table III. Here the ratios of strengths relative to the 6023 Å line are 0.27, 1.0, 0.32, 0.48, and 0.64. No fluorescence was observed when scanning from 6220 to 6290 Å $\left(Nd^{3+}\left({}^2H_{11/2} - {}^4I_{9/2}\right)\right)$ and from 7170 to 7230 Å $\left(Nd^{3+}\left({}^2H_{11/2} - {}^4I_{11/2}\right)\right)$ to greater than 1.2 times the background level, even when pumping ions directly to the ${}^2H_{11/2}$ level (6630 Å).

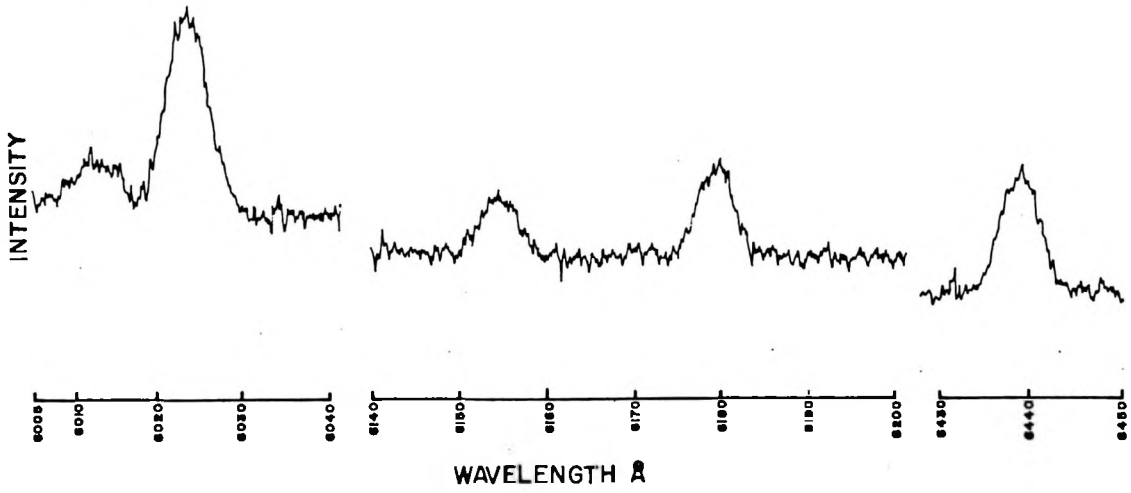


Figure 18. Fluorescence from $Pr:LaCl_3$ at 4.2°K under 32,000 $cm^{-1}$ excitation.

c. 1%Ho: 1%Pr: $LaCl_3$ Polycrystalline Sample at 4.2°K

The 1% double doped sample was excited with photons of approximately 32,000 $cm^{-1}$ energy. The fluorescence lines observed were assignable to $Ho^{3+}$ or to $Pr^{3+}$ transitions.

The fluorescence lines observed at about 4856, 4871, 4877, 4891, and 4906 Å had a signal strength above background relative to the 4877 Å line of 0.12, 0.97, 1.0, 0.62, and 0.71, with a background level of 0.23 and a noise level of 0.05. These fluorescence lines were identified as due to $Ho^{3+}$ transitions $^5F_3 - {}^5I_8$. There was no fluorescence in the vicinity of 4841 Å within a factor of 1.1 times the background level. A trace of the fluorescence reported can be seen in Figure 16 and Table III. The only other fluorescence traceable to $Ho^{3+}$ was observed at approximately 6454, 6467, 6476, 6483, and 6492 Å, with relative strengths above the background of 0.08, 0.22, 0.78, 0.92, and 1.0, with a background level of 0.34 and a noise level of from 0.16 to 0.31 (these numbers represent the average of three runs) (see Table II). This group of lines was assigned to the $Ho^{3+}$ transitions $^5F_3 - {}^5I_7$ and $^5F_5 - {}^5I_8$. The $Ho^{3+}$ fluorescence observed in this group was roughly twice as strong as that in the powder sample Ho: $LaCl_3$ under the same conditions. This does not

take into account loss of excitation in the nearly transparent polycrystalline sample, but does take into account the changes in the amplifier and photomultiplier gain between the two experiments. A broad line was also observed at approximately 6447 Å, with a relative strength of 0.50. A possible identity of this line will be discussed in Chapter IV.

When the strength of the 4877 Å line in Ho: Pr: $LaCl_3$ under 32,000 $cm^{-1}$ excitation (Figure 16c) was compared with the same line in Ho: $LaCl_3$ under $^5G_6$ excitation (Figure 16b), it was found to be weaker by a factor of approximately 300. This was arrived at by considering the relative line heights, the gains of the photomultiplier and amplifier in the two experiments, and the difference in the output of the mercury lamp at the two excitation energies. Again, the factor does not take into account the loss of excitation in the polycrystalline double doped sample.

Fluorescence which will be attributed to $Pr^{3+}$ transitions was observed at approximately 6023, 6154, 6179, and 6440 Å, with strengths above the background, relative to the 6023 Å line, of 1.0, 0.3, 0.45, and 0.14 with a background level of 0.48 and a noise level of 0.33 (these numbers represent the averages of two

runs made after long immersion in the dewar) (see Table IV). The first line of this group was attributed to the $Pr^{3+}$ transition $^1D_2 - {}^3H_4$, the next two to $^3P_0 - {}^3H_6$, and the last to $^3P_0 - {}^3F_2$. A trace of the fluorescence spectrum observed is shown in Figure 19. $Pr^{3+}\left(^1G_4 - {}^3H_4\right)$ fluorescence was searched for from 1.007 $\mu$ to 1.027 $\mu$, but none was observed to within 1.15 times the background even when pumping ions to the $Pr^{3+}\left(^3P_0\right)$ level, and no fluorescence which would correspond to the $^3P_0 - {}^1G_4$ transition was seen. $Pr^{3+}\left(^3F_3 - {}^3H_4\right)$ fluorescence was searched for from 1.57 to 1.594 $\mu$, but none was observed to within 1.15 times the background, even when pumping ions to the $Pr^{3+}\left(^3P_1\right)$ level. Fluorescence corresponding to the transition $^3P_1 - {}^3F_3$ was observed when exciting ions directly to the $^3P_1$ level, but no fluorescence from ions at the $^3F_3$ level was observed.

d. 1%Ho: 1%Nd: $LaCl_3$ Polycrystalline Sample at 4.2°K

The 1% double doped sample was excited at 32,000 $cm^{-1}$ and weak fluorescence was observed from 6440 to 6520 Å, with a very broad peak at approximately 6457 Å which was attributed to the $Nd^{3+}$ transition $^4D_{3/2} - {}^4F_{5/2}$. Within the broad background fluorescence leading up to the 6457 Å line, unresolved structure could be seen, but the noise level prevented identification of

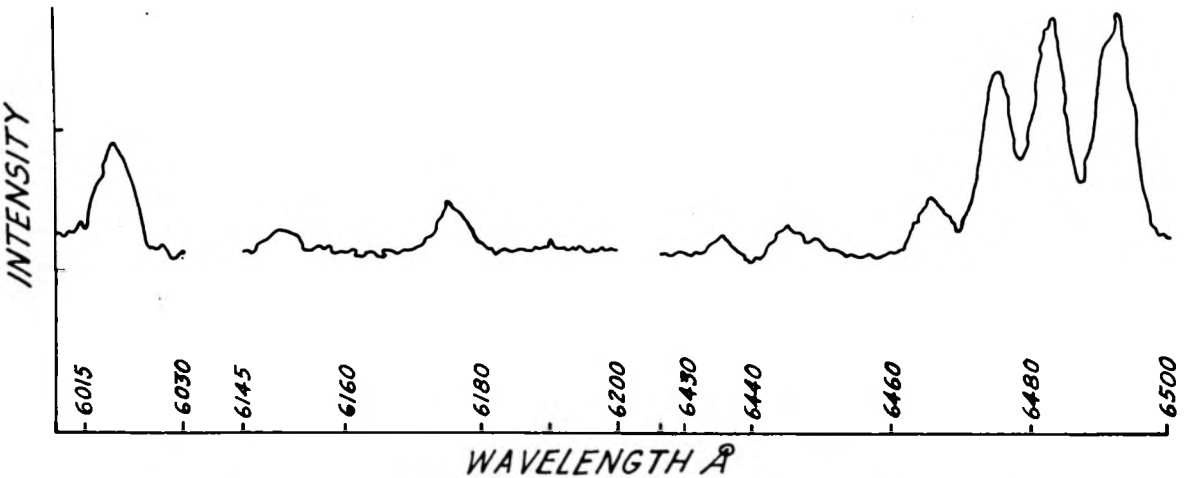


Figure 19. Fluorescence from Ho:Pr:$LaCl_3$ at 4.2°K under 32,000 $cm^{-1}$ excitation.

individual lines. This broad fluorescence, which was attributed to the $Ho^{3+}$ transition $^5F_5 - {}^5I_8$, is shown in Figure 14. A broad peak of fluorescence was also observed at approximately 5935 Å, shown in Figure 14, which was attributed to the $Nd^{3+}$ transition $^4G_{5/2} - {}^4I_{9/2}$.

4. Absorption Measurements

Photographic absorption measurements from 2900 to 3880 Å were made on all of the single crystal and polycrystalline samples at 4.2°K. No absorption lines were observed in the vicinity of 32,000 $cm^{-1}$ in any sample. All of the $LaCl_3$ samples examined (1%Pr, 1% Ho, and 1%Pr + 1%Ho) showed at least three $Nd^{3+}$ single ion absorption lines, at 27,976 $cm^{-1}$, 27,980 $cm^{-1}$, and 28,517 $cm^{-1}$. Following Carlson,[43] these lines were assigned to the $Nd^{3+}$ levels $^4D_{3/2}$ (1), $^4D_{3/2}$ (2), and $^4D_{1/2}$ (5), where the numbers in parentheses refer to crystal field quantum numbers. If one examines the densitometer trace given by Dieke and Dorman,[2] it can be seen that even in 100% $PrCl_3$, the strongest ion pair absorption lines there were weaker by about a factor of 1.4 than those due to trace amounts of $Nd^{3+}$.

5. Excitation Measurements

a. Unnormalized Excitation Spectra

Excitation spectra were taken of all of the $Pr^{3+}$ and $Ho^{3+}$ fluorescence lines thought to be involved in the pair processes, both in the $Ho^{3+} + Pr^{3+}$ double doped crystal as well as in Ho: $LaCl_3$ and Pr: $LaCl_3$. The excitation spectra of the double doped sample actually showed a minimum of excitation in the region of interest ($\sim$ 32,000 $cm^{-1}$), which, it was hypothesized, was due to variations in the output of the AH-6 mercury lamp as a function of wavelength. Although the excitation spectrum of the $Ho^{3+}$ level $^5F_5$ showed the same structure as reported by Porter,[17] it was impossible to tell without taking the ratio of output to input whether the small peak at 3131 Å was due to the weak mercury line exciting the continuum radiation reported by Edwards and Porter,[39, 40] or whether it was due to an actual two ion process. It was thus evident that unless the spectral distribution of the mercury lamp could be compensated for, excitation spectra could not yield proof of the existence of the two ion absorption process, since its excitation was much less than the spectral variation of the lamp in the same region. At the same time, however, the expected excitation spectra of the $Ho^{3+}$ levels showed that the equipment and

technique were working normally. For this reason, all further excitation measurements were made with the normalized excitation equipment described in Chapter II, section 7.

b. Normalized Excitation Spectra: 1%Pr: $LaCl_3$ at 4.2°K

Normalized excitation spectra were taken of the fluorescence from two different $Pr^{3+}$ levels in the 1%$Pr^{3+}$ doped sample. The first fluorescence monitored was that from ions at the $^1D_2$ level. Broad excitation was observed around 2700 Å, from 2860 to 3040 Å with a peak at 2960 Å, around 3110 Å, and around 3300 Å. These peaks were all quite broad, with the 2700 and 3300 Å peaks undergoing radical changes of strength, apparently with the heating and cooling history of the crystal. In one case, the 3300 Å line changed its strength relative to an adjacent (and fairly constant) line by a factor of approximately 12.5. The 3100 Å peak was the weakest peak in most cases, typically about 1/2 the size of the broad 2860-3040 peak. The assignment of processes to these excitation lines will be left to Chapter IV. This excitation spectrum is shown in Figure 20.

The next $Pr^{3+}$ fluorescence monitored was that corresponding to the transition $^3P_0 - {}^3H_6$. This transition showed peaks of excitation at approximately 2780, 3100, and 3400 Å, with radical changes in

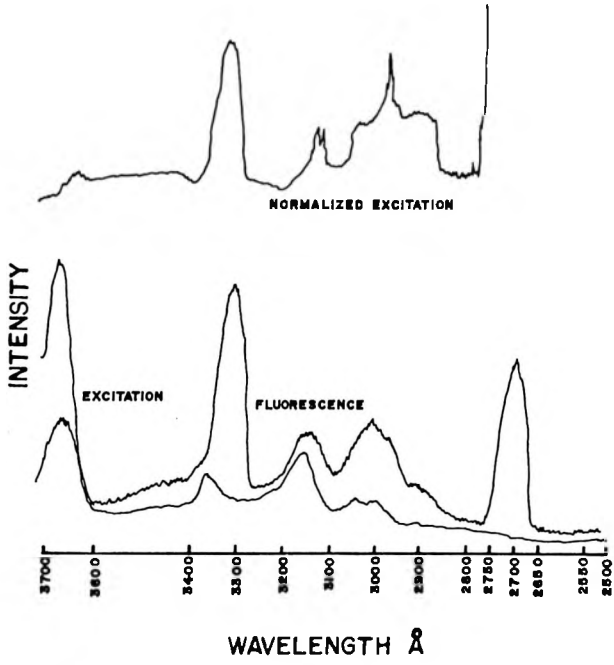


Figure 20. Normalized excitation spectrum of the transition $^1D_2$- $^3H_4$ in Pr:$LaCl_3$ at 4.2°K.

the strengths of all but the 3100 Å line. When the fluorescence from the transition $^3P_0 - {}^3H_4$ was monitored, excitation peaks were observed at approximately 2670, and 3100 Å, with changes in strength of the 2670 Å line by a factor of more than 12, again, apparently due to the heating and cooling history of the crystal. In both cases, the 3100 Å excitation was the smallest peak observed. When the excitation source was set on the strong excitation peaks, and the fluorescence produced was scanned, it was observed that in several cases, the peak of fluorescence was not on the expected $Pr^{3+}$ transition, but was shifted, by up to 25 Å, to peaks which were, in some cases, identifiable as $Nd^{3+}$ transitions. The fluorescence produced by the 3100 Å excitation always peaked on a $Pr^{3+}$ transition. These excitation spectra are shown in Figures 21 and 22. No excitation peaks were observed that could be unambiguously assigned to excitation energies corresponding to Pr + Pr ion pair absorption. This will be discussed in Chapter IV.

c. Normalized Excitation Spectra: 1%Ho: $LaCl_3$ at 4.2°K

Excitation spectra were made of the fluorescence from the transition $^5F_3 - {}^5I_8$, and from the largest peaks in the group containing both the $^5F_5 - {}^5I_8$ and the $^5F_3 - {}^5I_7$ transitions. Both of

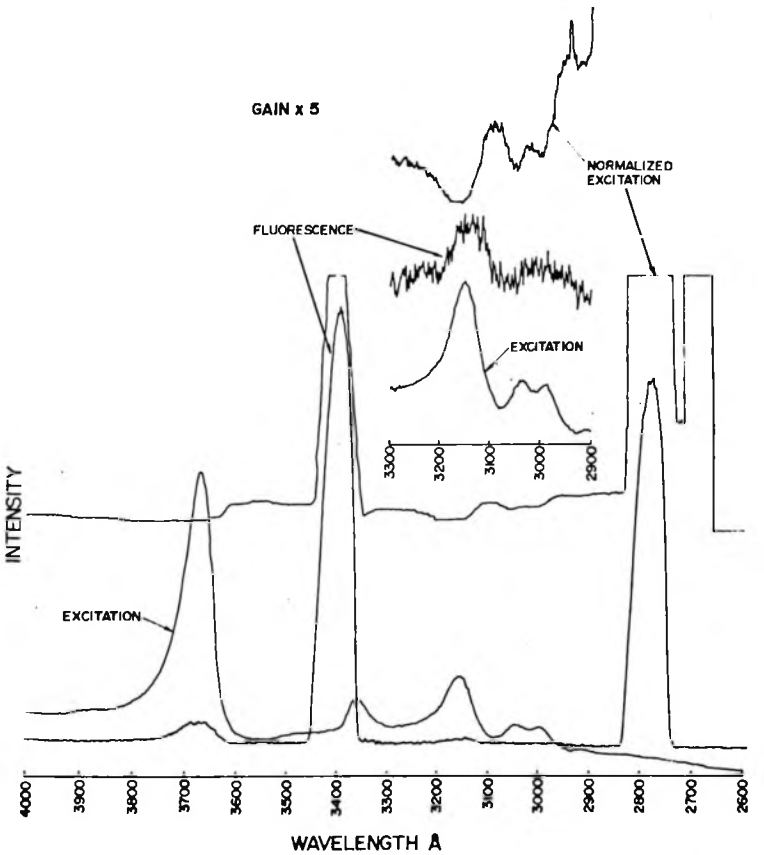


Figure 21. Normalized excitation spectrum of the transition $^3P_0 - {}^3H_6$ in $Pr:LaCl_3$ at 4.2°K.

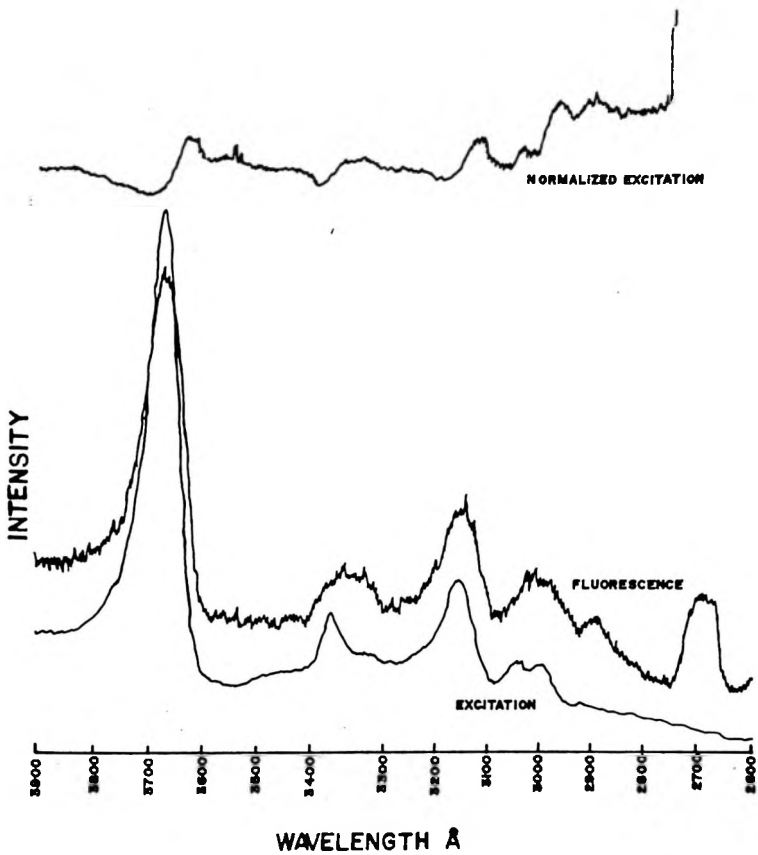


Figure 22. Normalized excitation spectrum of the transition $^3P_0 - {}^3H_4$ in $Pr:LaCl_3$ at 4.2°K.

these spectra showed excitation from all the levels reported by Porter,[17] but the small peak of signal near 3100 Å observed for the strongest line in the group $^5F_5 - {}^5I_8$ and $^5F_3 - {}^5I_7$ was shown to include a true peak of excitation, and not to be due completely to the nearby mercury lamp peak. The peak at 3100 Å was only observed for the group whose wavelength range included the $^5F_5 - {}^5I_8$ and $^5F_3 - {}^5I_7$ transitions.

The $^5F_3 - {}^5I_8$ fluorescence did not show any peak at 32,000 $cm^{-1}$ excitation energy. No excitation was observed at wavelengths which correspond to Ho + Ho pair absorption over the range of 2800 - 3800 Å. These spectra are shown in Figure 23 for the region from 2900 to 3300 Å.

d. Normalized Excitation Spectra: 1%Ho: 1%Pr: $LaCl_3$ at 4.2°K

The excitation spectrum for the $Pr^{3+}$ transition $^3P_0 - {}^3H_4$ was similar to that obtained with the single doped sample; a peak at approximately 3100 Å was observed, and the other larger peaks varied considerably in strength from run to run, which will be attributed to the heating and cooling of the crystal. The $^3P_0 - {}^3H_4$ excitation spectrum can be seen in Figure 24. The same comments apply to the spectrum due to the $Pr^{3+}$ transition $^1D_2 - {}^3H_4$; again the 3100 Å peak was observed. This spectrum can be seen in Figure 25.

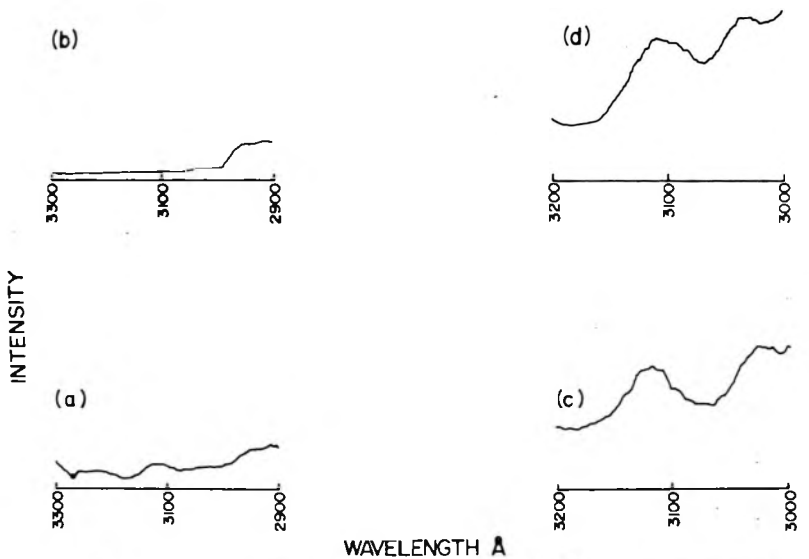


Figure 23. Normalized excitation spectra at 4.2°K in the vicinity of 32,000 $cm^{-1}$ for the transition

(a) $^5F_5$ - $^5I_8$ in Ho:$LaCl_3$, (b) $^5F_3$ - $^5I_8$ in Ho:$LaCl_3$

(c) $^5F_5$ - $^5I_8$ in Ho:Pr:$LaCl_3$, (d) $^5F_3$ - $^5I_8$ in Ho:Pr:$LaCl_3$.

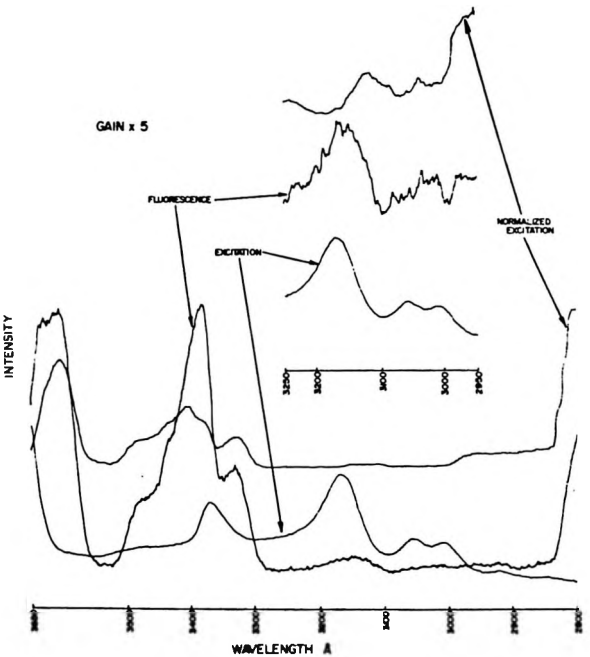


Figure 24. Normalized excitation spectrum of the transition $^3P_0 - {}^3H_4$ in Ho:Pr:$LaCl_3$ at 4.2°K.

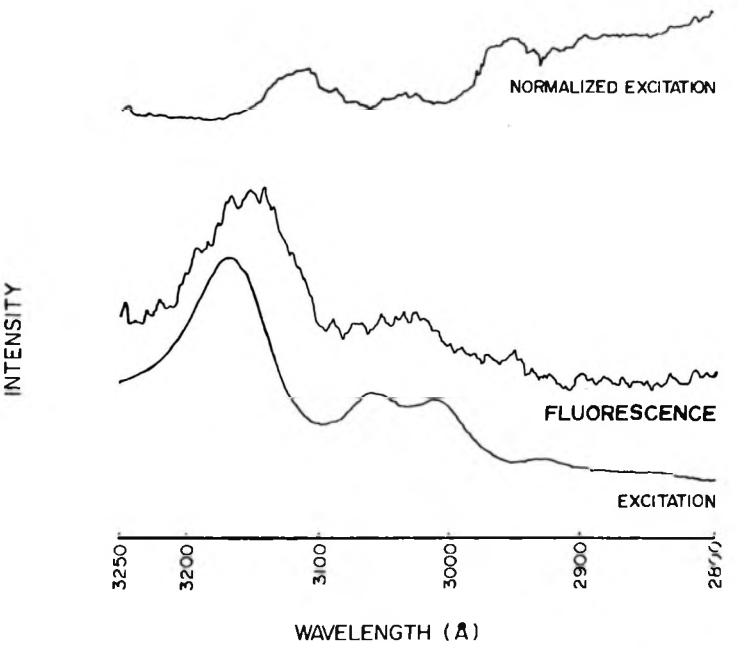


Figure 25. Normalized excitation spectrum of the transition $^1D_2 - {}^3H_4$ in Ho:Pr:$LaCl_3$ at 4.2°K.

The excitation spectrum for both $Ho^{3+}$ transitions was the same as that observed for the single doped sample with the exception that in the double doped crystal, the transition $^5F_3 - {}^5I_8$ showed a peak of excitation at 3100 Å, while it did not in the single doped crystal. These spectra are shown in Figure 23 for the region from 3000 to 3200 Å.

# CHAPTER IV

# DISCUSSION

## 1. Introduction

In an effort to see if pairs of ions dilutely dispersed in a crystal could absorb a single photon, as has been observed in high concentrations, the fluorescence spectra of 1%$Ho^{3+}$, 1%$Pr^{3+}$, and 1%$Ho^{3+}$ + 1%$Pr^{3+}$ in $LaCl_3$ were examined at 4.2°K and approximately 32,000 $cm^{-1}$ excitation. Results have been presented in Chapter III. The following ion pair absorption processes involving these elements plus $Nd^{3+}$, present as an impurity, are energetically possible in the excitation range of from 31,939 $cm^{-1}$ to 32,584 $cm^{-1}$ (from Table I):

(1) $Ho^{3+}\left(^5F_5\right) + Pr^{3+}\left(^1D_2\right)$

(2) $Ho^{3+}\left(^5G_6\right) + Pr^{3+}\left(^1G_4\right)$

(3) $Ho^{3+}\left(^5G_4\right) + Pr^{3+}\left(^3F_3\right)$

(5) $Ho^{3+}\left(^5G_5\right) + Ho^{3+}\left(^5I_6\right)$

(6) $Pr^{3+}\left(^3P_2\right) + Pr^{3+}\left(^1G_4\right)$

(7) $Pr^{3+}\left({}^3P_0\right) + Nd^{3+}\left({}^4F_{3/2}\right)$

(8) $Pr^{3+}\left({}^3P_1\right) + Nd^{3+}\left({}^4F_{3/2}\right)$

(9) $Pr^{3+}\left({}^1D_2\right) + Nd^{3+}\left({}^2H_{11/2}\right)$

(12) $Ho^{3+}\left({}^5G_2\right) + Nd^{3+}\left({}^4I_{13/2}\right)$

(13) $Ho^{3+}\left({}^3K_7\right) + Nd^{3+}\left({}^4I_{15/2}\right)$

(14) $Ho^{3+}\left({}^3H_6\right) + Nd^{3+}\left({}^4I_{13/2}\right)$

(15) $Ho^{3+}\left({}^5F_2\right) + Nd^{3+}\left({}^4F_{3/2}\right)$

(16) $Ho^{3+}\left({}^5F_5\right) + Nd^{3+}\left({}^4G_{5/2}\right)$

(Note: Only pair processes have been included which involve $Ho^{3+}$ levels higher than or equal to the ${}^5F_5$ level in energy and $Pr^{3+}$ levels higher than or equal to the ${}^1D_2$ level in energy.)

One of the conditions for observing ion pair absorption is that there be no single ion levels in the vicinity of 32,000 $cm^{-1}$. As can be seen in Figures 1 and 2, the closest $Nd^{3+}$ levels are the ${}^2H_{9/2}$ (approximately 31,500 $cm^{-1}$) and the ${}^4D_{3/2}$ (approximately 32,800 $cm^{-1}$), while the $Ho^{3+}$ levels nearby are the ${}^3D_2$ (30,747 $cm^{-1}$) and the ${}^3D_3$ (2) (33,056 $cm^{-1}$), and the nearest $Pr^{3+}$ levels are the ${}^3P_2$ (2) (22,747 $cm^{-1}$)

and the $^1S_0$ (0)(approximately 48,800 $cm^{-1}$). It is thus possible to pump energy into the crystal at approximately 32,000 $cm^{-1}$ without exciting any single ion.

2. 1%Ho: $LaCl_3$

When the powder crystal 1%Ho: $LaCl_3$ fluorescence was examined under 32,000 $cm^{-1}$ excitation, a group of lines was observed between 6454 and 6520 Å, but no fluorescence was seen from 4860 to 4910 Å. The first group is in the wavelength range of the $^5F_3$ - $^5I_7$ and $^5F_5$ - $^5I_8$ transitions, while the second range corresponds to $^5F_3$ - $^5I_8$ transitions. Since no $^5F_3$ to ground transitions were observed, one can deduce that the group of six lines observed from 6454 to 6513 Å corresponds solely to transitions from $^5F_5$ to $^5I_8$. This is verified by the different relative intensities of the group under 32,000 $cm^{-1}$ excitation when compared with the relative intensities of the same group under direct $^5F_3$ excitation. The ratios of the lines for the 32,000 $cm^{-1}$ excitation are 0.32, 0.55, 0.49, 0.82, 1.0, and 0.47, while for the direct $^5F_3$ excitation, the ratios are 0.28, 0.56, 1.05, 1.14, 1.0, and 0.23. This comparison is shown in Figures 14b, 15b and Table II. Excitation spectra of the $Ho^{3+}(^5F_5)$ and $^5F_3$

transitions to ground for 1%Ho: $LaCl_3$ verify these results: the transition $^5F_5 - {}^5I_8$ has a peak of excitation at 32,000 $cm^{-1}$; the transition $^5F_3 - {}^5I_8$ does not. This can be seen in Figure 23a, b.

Excitation of ions to the $Ho^{3+}\left(^5F_5\right)$ level by an ion pair absorption with the $Nd^{3+}$ level $^4G_{5/2}$ (process (16) above) is energetically possible at 32,000 $cm^{-1}$. In fact, fluorescence was observed for the transitions from the $Nd^{3+}$ level $^4G_{5/2}$ to the ground level $^4I_{9/2}$ and to the first excited level $^4I_{11/2}$ when the sample was pumped at 32,000 $cm^{-1}$. This fluorescence can be seen in Figure 14b,c. The identity of these transitions was established by the use of Carlson's[43] results. In addition, these transitions were observed by directly pumping to higher levels in a crystal containing 1%Ho + 1%Nd in $LaCl_3$. This double doped crystal was also pumped at 32,000 $cm^{-1}$ to check the two ion absorption process as described in Chapter III, section 3d. Fluorescence was observed which was attributed to ions at the $Nd^{3+}$ level $^4G_{5/2}$, and some weak fluorescence was also observed in the area where the $Ho^{3+}\left(^5F_5\right)$ transitions should lie, but these transitions lie in the tail of an extremely broad $Nd^{3+}$ line coming from the transition $^4D_{3/2} - {}^4F_{5/2}$. It is possible that ions at the $^4D_{3/2}$ level are excited by a pair with ions at the $Nd^{3+}$ level

$^4I_{13/2}$, (the energy sum is 31,895 to 32,059 $cm^{-1}$), but the fluorescence from $^4I_{13/2}$ to ground was not searched for. Figure 14a shows the fluorescence observed from the double doped crystal.

Fluorescence from the $Ho^{3+}$ level $^5G_5$ (Process (5)) was not searched for, as this level is not connected by decay processes with the $^5F_3$ or $^5F_5$ levels. Fluorescence from $Ho^{3+}$ levels other than the $^5F_5$ involved in the Ho + Nd ion pair processes (12 - 15) was not searched for, as ions in all of these levels decay to the $^5F_3$ level, and the $^5F_3$ level was not observed to fluoresce under 32,000 $cm^{-1}$ excitation.

3. 1%Pr: $LaCl_3$

The next sample examined for fluorescence with 32,000 $cm^{-1}$ excitation was the 1%$Pr^{3+}$: $LaCl_3$ single crystal. Fluorescence was observed which corresponded to electronic transitions from the levels $^1D_2$ and $^3P_0$. Although the relative intensities of the two $^1D_2$ lines remained constant, as did the relative intensitities of the three $^3P_0$ lines, the relative intensity of any $^1D_2$ line to any $^3P_0$ line changed radically, apparently as a function of the time the sample spent in the dewar of liquid helium. Shortly after immersion, the ratio of $^1D_2$

peak fluorescence to that from $^3P_0$ was roughly the same or very slightly higher than when ions were excited to the $^1D_2$ level by decay from the $^3P_2$, $^3P_1$, and $^3P_0$ levels. When ions are excited to the $^3P_2$ level, the ratio of the $^1D_2$ (6023 Å) line to the $^3P_0$ (6440 Å) line was 0.06 to 1, while at 32,000 $cm^{-1}$ excitation and shortly after immersion in the helium, the ratio was 0.3 to 1. After several hours, the ratio was 2.77 to 1. The absolute strength of the $^3P_0$ fluorescence did not change significantly during this time. What this implies is that immediately after immersion in the liquid helium, the primary means of exciting ions to the $^1D_2$ level was by decay from the $^3P_0$ level; after some time, the excitation came from some mechanism other than decay from $^3P_0$. At 32,000 $cm^{-1}$ excitation, a possible mechanism for causing $^3P_0$ fluorescence would be the pair absorption $Pr\left(^3P_2\right) + Pr\left(^1G_4\right)$ (process (6) above), while the separate $^1D_2$ fluorescence could be caused by the pair absorption $Pr\left(^1D_2\right) + Nd\left(^2H_{11/2}\right)$ (process (9) above). Since, even immediately after immersion, there seems to be slightly more $^1D_2$ fluorescence than could be explained strictly by decay from ions at the $^3P_0$ level, processes (9) and (6) are probably both operating all the time, but with process (9) getting stronger with long immersion times in the dewar.

After about two hours, the process appears to reach its maximum strength, which is approximately 13 times stronger than right after immersion, and remains at this strength as long as helium remains in the dewar. As the dewar heats up after helium evaporation, the strength of the $^1D_2$ fluorescence decreases.

The $Nd^{3+}$ fluorescence from ions at the $^2H_{11/2}$ level was not observed, even under direct excitation. Carlson[43] reports that fluorescence originating from $Nd^{3+}$ ions excited to this level is extremely weak at 4.2°K. The presence of $Nd^{3+}$ as an impurity was verified by the appearance of $Nd^{3+}$ absorption lines in the photographic absorption spectrum made with the 1%$Pr^{3+}$ doped $LaCl_3$ crystal.

The excitation spectra for the $^3P_0$ and $^1D_2$ transitions in the $Pr^{3+}$ single doped crystal were similar in that they both showed peaks of excitation at 32,000 $cm^{-1}$ (see Figures 20 and 21). In addition, they both showed other excitation peaks that varied enormously in intensity, apparently due to the heating and cooling history of the crystal. This behavior appeared to be similar to the liquid helium immersion time dependence observed for the $^1D_2$ fluorescence in the same sample, and which has been related to a pair process involving

trace amounts of $Nd^{3+}$. When the excitation peaks were at their strongest, they were comparable to the stronger single ion excitation peaks observed in the Ho: $LaCl_3$ sample, but there were no known $Pr^{3+}$ single ion levels in the vicinity. A clue to this puzzle was provided by the fact that in several cases, the fluorescence produced by these strong excitations was not peaked on the $Pr^{3+}$ fluorescence line being monitored, but was shifted by up to 25 Å, to lines that were identified as $Nd^{3+}$ transitions. This fact implies that the excitation peaks observed are actually single ion $Nd^{3+}$ excitations, producing strong $Nd^{3+}$ fluorescence, the tail of which includes wavelengths corresponding to the $Pr^{3+}$ transitions being monitored. This is supported by the fact that except for the excitation at 32,000 $cm^{-1}$ ($\sim$ 3100 Å), the excitation spectra of the fluorescence transitions $^3P_0 - {}^3H_4$ and $^3P_0 - {}^3H_6$ have little in common. The major peaks of excitation fall at significantly different wavelengths, but if these peaks represented true excitation of ions to the $^3P_0$ level, the spectra should be the same. Thus, it can be concluded that these peaks represent excitation of some fluorescent transition which overlaps the $^3P_0$ transitions, but is not related to them. Table VI presents the proposed assignments of the observed $Pr^{3+}$ excitation spectra based

Table VI.

Tentative Assignments of $Pr^{3+}$ Excitation Peaks.

(a) $^1D_2$ - $^3H_4$ Transition Monitored (6023Å)

| Fluorescence Peak/Assignment | Excitation Peak/Assignment | Comments |
|---|---|---|
| 6052Å<br>$Nd^{3+}$ $(^4D_{3/2}$ - $^4F_{3/2})$ | 2700Å<br>$Nd^{3+}$ Level (?) at 2,692Å (est.) | Strong, but variable, sometimes largest peak |
| 6023Å<br>$Pr^{3+}$ $(^1D_2$ - $^3H_4)$ | 2700Å<br>$Pr^{3+}$ $(^3P_0 + {}^1D_2)$ | Energetically possible, but should be weak |
| 6023Å<br>$Nd^{3+}$ $(^4D_{3/2}$ - $^4F_{3/2})$ | 2860 - 3040Å<br>$Nd^{3+}$ $(^2H_{11/2})$ (2932 - 2947Å) (est.)<br>$Nd^{3+}$ $(^2D_{5/2})$ (3017Å) (est.)<br>$Pr^{3+}$ $(2X\ {}^1D_2)$ (3000Å)<br>peak at 2960Å | Fairly constant overall peak<br>Energetically possible |
| 6023Å<br>$Pr^{3+}$ $(^1D_2$ - $^3H_4)$ | 3100 - 3120Å<br>$Pr^{3+}$ $(^3P_2 + {}^1G_4)$<br>$Pr^{3+}$ $(^1D_2)$ + $Nd^{3+}$ $(^2H_{11/2})$<br>$Pr^{3+}$ $(^3P_0)$ + $Nd^{3+}$ $(^4F_{3/2})$<br>$Pr^{3+}$ $(^3P_1)$ + $Nd^{3+}$ $(^4F_{3/2})$ | Constant, but weak |
| 6046Å<br>$Nd^{3+}$ $(^4D_{3/2}$ - $^4F_{3/2})$ | 3300Å<br>$Nd^{3+}$ $(^2I_{13/2})$ | Strong, but variable |
| 6023Å<br>$Pr^{3+}$ $(^1D_2$ - $^3H_4)$ | $Pr^{3+}$ $(^3P_0 + {}^1G_4)$ | Possible |

Table VI. Tentative Assignments of $Pr^{3+}$ Excitation Peaks (cont.).

(b) $^3P_0 - {}^3H_6$ Transition Monitored (6181Å)

| Fluorescence Peak/Assignment | Excitation Peak/Assignment | Comments |
|---|---|---|
| 6188Å<br>$Nd^{3+}\left({}^2H_{11/2} - {}^4I_{9/2}\right)$(6280Å) ? | 2780Å | Very strong, variable |
| 6181Å<br>$Pr^{3+}\left({}^3P_0 - {}^3H_6\right)$ | 3100Å<br>$Pr^{3+}\left({}^3P_2 + {}^1G_4\right)$ | Weak, but constant |
| 6189Å<br>$Nd^{3+}\left({}^2H_{11/2} - {}^4I_{9/2}\right)$(6280Å) ? | 3400Å<br>$Nd^{3+}\left({}^2L_{15/2}\right)$ | Strong, but variable |

(c) $^3P_0 - {}^3H_4$ Transition Monitored (4891 Å)

| Fluorescence Peak/Assignment | Excitation Peak/Assignment | Comments |
|---|---|---|
| 4891Å<br>$Nd^{3+}\left({}^4G_{9/2} - {}^4I_{9/2}\right)$(4820Å) ? | 2670 - 2680Å<br>$Nd^{3+}$ level (?) at 2692Å | Strong, but variable |
| 4891Å<br>$Pr^{3+}\left({}^3P_0 - {}^3H_4\right)$ | 3100Å<br>$Pr^{3+}\left({}^3P_2 + {}^1G_4\right)$ | Weak, but constant |

on this explanation, but including energetically possible Pr + Pr ion pair absorption processes.

4. 1%Ho: 1%Pr: $LaCl_3$

Finally the fluorescence from the 1%Ho: 1%Pr: $LaCl_3$ polycrystalline sample was examined under 32,000 $cm^{-1}$ excitation. The $Ho^{3+}$ fluorescence observed corresponded to the transition $^5F_3 - {}^5I_8$, and to the group $^5F_3 - {}^5I_7$ and $^5F_5 - {}^5I_8$. The ratios of relative intensities in the latter group indicate that most, but not all, of the $^5F_5$ excitation was due to ions decaying from the $^5F_3$ level. The latter group was also at least twice as intense as the same group in the Ho: $LaCl_3$ powdered sample under 32,000 $cm^{-1}$ excitation. A comparison of those fluorescence groups can be seen in Figure 15. The $^5F_3$ fluorescence was quite strong, but no radiation was observed from the $^5G_4$ level, indicating that the $^5F_3$ level was not pumped by ions descending from the $^5G_4$ level. A comparison of the $^5G_4 - {}^5I_7$ and $^5F_3 - {}^5I_8$ fluorescence groups for the double doped crystal and the 1%Ho: $LaCl_3$ sample under direct excitation of ions to the $^5G_4$ and $^5G_6$ levels is shown in Figure 16. The identity of the line at 6447 Å is in question, but its wavelength does correspond to the $Nd^{3+}$ transition $^4D_{3/2}$ to $^4F_{3/2}$.

The normalized excitation spectra for the $^5F_3$ and $^5F_5$ fluorescence showed the normal $Ho^{3+}$ excitation structure reported by Porter[17], and, in addition, both fluorescence lines exhibited peaks of excitation at 32,000 $cm^{-1}$. These peaks are shown in Figure 23c, d.

The $Pr^{3+}$ fluorescence observed under 32,000 $cm^{-1}$ excitation was assigned to the $^1D_2$ and $^3P_0$ levels. If the $^3P_0$ level is excited, fluorescence weaker than from $^3P_0$ is also observed from the $^1D_2$ level. As noted in Chapter III, section 3c, the fluorescence from the $^1D_2$ level always dominated under 32,000 $cm^{-1}$ excitation. Therefore, the ions were being excited to the $^1D_2$ level by some mechanism other than decay from the $^3P_0$ level. The ratio of $^1D_2$ to $^3P_0$ fluorescence did not change significantly with immersion time in the dewar or whether the crystal was used several days in succession or allowed to rest for a week. Fluorescence corresponding to the transitions $^1G_4 - {}^3H_4$ and $^3F_3 - {}^3H_4$ was not observed, even when populating the upper levels directly. This radiation has not been reported in the literature, although Moos[42] indicates that both levels do fluoresce in $LaCl_3$.

Finally, examination of the excitation spectra of the $Pr^{3+}$ transitions from ions at the $^1D_2$ and the $^3P_0$ levels showed the same peaks

of excitation as exhibited by the 1%Pr: $LaCl_3$ sample, including peaks at 32,000 $cm^{-1}$ excitation for both fluorescence lines. In addition, the absorption specturm of the double doped sample showed three lines which were identified as due to $Nd^{3+}$ impurities.

5. Synopsis

Referring to the list of possible ion pair absorption processes given in the beginning of this chapter, one can make the following deductions from the data:

1. In the $Ho^{3+}$ doped crystal, the Ho + Nd ion pair absorption process (16) is operative at 32,000 $cm^{-1}$ excitation, involving trace amounts of $Nd^{3+}$, and this results in the excitation of ions to the $^5F_5$ level but not to the $^5F_3$ level. Evidence for this statement comes not only from the fluorescence, but also from the excitation data, since the $^5F_5$ level shows excitation at 32,000 $cm^{-1}$ while the $^5F_3$ level does not.

2. In the $Ho^{3+}$ doped crystal, no evidence was observed for Ho + Ho ion pair absorption.

3. In the $Pr^{3+}$ doped crystal, evidence was seen for the Pr + Nd ion pair absorption process (9) at 32,000 $cm^{-1}$ excitation,

and the strength of this process varied with length of time in the liquid helium filled dewar. The presence of the $Nd^{3+}$ in trace amounts was verified by absorption spectra. It is possible that the Pr + Pr ion pair absorption process (6) is also operating weakly, since there is a peak of excitation for the $^3P_0$ fluorescence at 32,000 $cm^{-1}$, even though the fluorescence from the $^1G_4$ level was not detected. There are, however, two combinations with $Nd^{3+}$ possible at this energy, processes (7) and (8). The $Nd^{3+}$ fluorescence for these processes was not searched for. All of the other excitation peaks indicated interactions with single ion $Nd^{3+}$ levels, but these strong peaks could have hidden some weak Pr + Pr ion pair excitation peaks, which were energetically possible.

4. In the $Ho^{3+}$ and $Pr^{3+}$ double doped crystal, evidence was seen for the Pr + Ho ion pair absorption as well as for the Ho + Nd, Pr + Nd, and possibly the Pr + Pr processes mentioned above. Of the three Ho + Pr processes proposed (1), (2), and (3), since no fluorescence was observed from the $Ho^{3+}\left(^5G_4\right)$ level, it can be concluded that process (3) is either extremely weak or is not operating at all. Since strong fluorescence was observed from the $^5F_3$ level in the double doped crystal at 32,000 $cm^{-1}$ excitation and none was

observed in the $Ho^{3+}$ single doped crystal under the same conditions, it can be concluded that process (2) was operating strongly. Process (2) involves excitation to the $^5F_3$ level by a multiphonon decay from the ions at the $^5G_6$ level. Although the $Pr^{3+}$ fluorescence associated with process (2) was not observed, the fact that the $Ho^{3+}$ fluorescence from the $^5F_3$ level showed excitation at 32,000 $cm^{-1}$ in the double doped crystal, while it showed none in the single $Ho^{3+}$ doped crystal indicates that the Ho + Pr pair absorption process (2) was indeed operating. The strength of the $Ho^{3+}\left(^5F_3 - {}^5I_8\right)$ fluorescence was weaker by a factor of approximately 300 when the $^5G_6$ level was being populated in the double doped sample by process (2) as compared to direct excitation of the $^5G_6$ level in the Ho: $LaCl_3$ sample. Finally, the fact that the $Pr^{3+}\left(^1D_2\right)$ fluorescence did not show a variation in strength relative to the $^3P_0$ fluorescence as a function of time in the dewar indicates that at least some of the $^1D_2$ excitation is coming from some other mechanism other than pairs with $Nd^{3+}$. Since the $Ho^{3+}\left(^5F_5\right)$ fluorescence is much stronger in the double doped crystal than in the single doped crystal, and the relative strengths of the lines in the $^5F_3 - {}^5I_7$ and $^5F_5 - {}^5I_8$ group are not quite the same as when the $^5F_5$ fluorescence is being produced

by decay from ions at the $^5F_3$ level, but show some of the features of the $^5F_5 - {}^5I_8$ group excited in the single doped crystal, it would seem reasonable to conclude that at least some of the $^5F_5$ excitation is being produced by some other mechanism other than pairs with $Nd^{3+}$ or by decay from ions at the $^5F_3$ level. A mechanism that would explain all of these data would be process (1), namely, an ion pair process involving the levels $Pr^{3+}\left(^1D_2\right)$ and $Ho^{3+}\left(^5F_5\right)$. Preliminary results pertaining to the Ho + Pr ion pair processes have been reported by Porter and Blatt.[45]

# CHAPTER V

# CONCLUSIONS AND RECOMMENDATIONS

## 1. Conclusions

Several fluorescence lines observed in dilutely doped $LaCl_3$ at $4.2^{\circ}K$ have been identified as being produced by the absorption of one photon by two dopant ions. Absorption by two dissimilar ions has been identified in 1%Ho: $LaCl_3$, 1%Pr: $LaCl_3$, and in 1%Ho: 1%Pr: $LaCl_3$. Absorption by pairs of similar ions may have been identified in 1%Pr: $LaCl_3$.

When the Ho: $LaCl_3$ crystal was pumped at approximately 32,000 $cm^{-1}$, where there are no single ion levels, $Ho^{3+}$ and $Nd^{3+}$ fluorescence was seen, which was attributed to the process $Ho\left({}^5F_5\right)+ Nd\left({}^4G_{5/2}\right)$. The Pr: $LaCl_3$ crystal was pumped under the same conditions, and fluorescence was seen which was attributed to the processes $Pr\left({}^1D_2\right)+ Nd\left({}^2H_{11/2}\right)$. Some ${}^3P_0$ fluorescence was also seen, but it was not detetmined whether this was due to a Pr + Pr or a Pr + Nd process, both of which are energetically possible. When the Ho: Pr: $LaCl_3$ crystal was pumped under the same conditions, the

process $Ho\left({}^5G_6\right) + Pr\left({}^1G_4\right)$ produced the strongest fluorescence, somewhat weaker fluorescence was attributed to the processes $Ho\left({}^5F_5\right) + Pr\left({}^1D_2\right)$ and $Ho\left({}^5F_5\right) + Nd\left({}^4G_{5/2}\right)$ plus $Pr\left({}^1D_2\right) + Nd\left({}^2H_{11/2}\right)$ and the third process $Ho\left({}^5G_4\right) + Pr\left({}^3F_3\right)$ is very weak, if, indeed it is operating at all. The fluorescence produced by the pair process $Ho\left({}^5G_6\right) + Pr\left({}^1G_4\right)$ in the double doped sample was weaker by a factor of approximately 300 than that produced in Ho: $LaCl_3$ by direct ${}^5G_6$ excitation. The pair processes involving $Nd^{3+}$ are attributed to trace amounts of $Nd^{3+}$, whose presence was verified in all crystals by photographic absorption measurements.

2. Recommendations for Future Work

In the process of this investigation several interesting facets of energy transfer processes were seen that could not be pursued in a systematic manner, although they were related to the principle problem under investigation. One of the most interesting of these topics was the extremely variable strength of some of the excitation peaks in the $Pr^{3+}$ excitation spectra. In addition, under 32,000 $cm^{-1}$ excitation, the ratio of the ${}^1D_2$ to ${}^3P_0$ fluorescence steadily grew, apparently with immersion time in the dewar. Both this process and the variable excitation peaks were attributed to $Nd^{3+}$ impurities, whose presence was

verified by photographic absorption measurements.

The variable interaction strength of an impurity dopant would be an extremely interesting topic of investigation by itself. Among the several approaches that could be followed are studies to see if the variation is due to the room temperature radiation impinging on the sample, studies of the effect of increasing the $Nd^{3+}$ content of the crystal, studies of the possible bleaching effect of radiation, and studies of the temperature dependence of the variation.

A second topic worthy of further investigation would be possible selection rules in an ion pair absorption process, especially between dissimilar ions. To obtain these selection rules, if they exist, it would be necessary to get high resolution absorption spectra. There are at least two approaches by which these might be obtained: First, a slight increase in the impurity concentration or in the length of the crystal might give enough absorption so that a trace on a photographic plate could be observed. This experiment could probably be performed most easily on Pr: $LaCl_3$, since all of the $Pr^{3+}$ single ion absorption lines are far away from 32,000 $cm^{-1}$. Second, the increased sensitivity and reduced noise of photoelectric measurements over photographic ones might provide the improvement necessary to see the absorption lines in 1% samples. To do this, it would probably

be necessary to build a high resolution double beam spectrometer, or at least to build a double beam attachment for an existing spectrometer, and use a differential amplifier to subtract the reference signal from the sample signal. An alternative to the higher noise level of a differential amplifier and the matching problems of two photomultipliers would be to build an optical chopper that alternates the beam through and around the sample, using an adjustable diaphragm to attenuate the reference beam, and phase separating the two signals with switching keyed by the chopper. The signals could then be subtracted with more confidence in the output since the same detector would be used for both channels. The optical layout for this second method would be complicated, but probably worth the added complexity.

The pursuit of the mechanism involved in ion pair absorption is important not only for the insight that it can give about how the ions interact with each other and the lattice, but also how the interaction of the ions with radiation is affected by the presence of adjacent ions, impurities, and the lattice itself.

# APPENDIX A

## NORMALIZED EXCITATION CIRCUIT DETAILS

If a weak pair process fluorescence is superimposed on a larger "continuum" or background fluorescence, a useful excitation spectrum of the pair process can be obtained by dividing the fluorescence output by the excitation output.

The theory behind the technique used is as follows: It is assumed that the fluorescence $I_f$ is the sum of two terms, $I_c$ due to any process which can be shown to vary slowly with excitation wavelength, and $I_{pp}$ due to the pair process. If $I_e$ is the excitation intensity, one can write

$$I_f = I_c + I_{pp} = \alpha_c(\lambda_e) I_e + \alpha_{pp}(\lambda_e) I_e \qquad (1)$$

where $\alpha_c(\lambda_e)$ is the coefficient of proportionality between the excitation and the fluorescence continuum intensities, and $\alpha_{pp}(\lambda_e)$ is the coefficient between the excitation and the pair process fluorescence intensitities. These are both written as functions of $\lambda_e$ since

it is assumed that the intensity of fluorescence due to both processes will be a function of the excitation wavelength. Naturally, $I_e$ is also a function of $\lambda_e$, due to the broad emission lines of the mercury lamp. If one then computes $I_f/I_e$, equation (1) becomes

$$I_f/I_e = \alpha_c(\lambda_e) + \alpha_{pp}(\lambda_e). \tag{2}$$

It is now assumed that $\alpha_c(\lambda_e)$ is such a slowly varying function of $\lambda_e$ that it can be considered essentially constant over a reasonable wavelength range. Equation (2) then becomes

$$I_f/I_e = \alpha_{pp}(\lambda_e) + C, \text{ where} \tag{3}$$

$C = \alpha_c$, assumed constant over a restricted range of $\lambda_e$. Since for sharp emission lines $\alpha_{pp}$ varies extremely rapidly with $\lambda_e$, a plot of $I_f/I_e$ versus $\lambda_e$ should give directly those values of $\lambda_e$ at which $\alpha_{pp}$ is non vanishing, or, in other words, those wavelengths at which the pair process is active. The justification for assuming that $\alpha_c$ is a constant comes from the work of Edwards and Porter,[39, 40] who found

that monochromatically excited $LaCl_3$ produces "continuum" radiation which is a slowly varying function of excitation wavelength. It is the variation of this "continuum" intensity with the source intensity that requires the normalization of the excitation spectrum.

A few words about the details of the circuit are in order at this point. The output of the PAR HR-8 lock-in amplifier is normally 0-0.5 v when operating with a center zero. In order to increase the operating range, a d.c. bias can be dialed in, placing the signal zero at one end of the scale, and giving an output of from -0.5 v to +0.5 v. Since convenience dictates a negative going output for a positive fluorescence input, an output range of +0.5 v to -0.5 v for both the fluorescence and the excitation outputs is used. Referring to Figure 13, it will be noticed that -0.5 v is added to both signals in the first operational amplifiers (#1 and 2) of the TR-10. This means that the signals effectively range from 0 to -1.0 v. If the original signals are labeled $I_f$ and $I_e$, these new signals are labeled $I_f'$ and $I_e'$. It can also be seen that this operation has no effect upon the ratio of the two intensities, since their original range was disposed equally about zero by dialing in a d.c. bias on the lock-in amplifier, and the above operation merely removes that bias.

One of the restrictions of using an analog divider is that if the two inputs are $I_f'$ and $I_e'$ and the output is $I_f'/I_e'$, then $I_e'$ must always be greater than or equal to $I_f'$, and $I_e'$ must never change sign (or go to zero). Again, referring to the schematic, it will be noticed that the first amplifier for the excitation signal (#2) has a gain of 10, while all the others (except for the divider network itself) have gains of one. This means that the divider gets inputs of $I_f'$ and $10\ I_e'$. A characteristic of this particular divider is that if the inputs are $I_f'$ and $10\ I_e'$ the actual output is $10\ I_f'/10\ I_e'$. Thus an output of $10\ I_f'/10\ I_e' = I_f'/I_e'$ is obtained with proper operation as long as $I_e$ is greater than or equal to $0.1\ I_f$, and, of course, as long as $I_e$ is greater than zero. In effect, this restricts the system to wavelengths longer than 2600 - 2850 Å, since below this value, the thermocouple output is too low if the gain is set to a useful level for a scan from 3000 to 4000 Å. An additional problem is that since the divider network is essentially a quarter-square multiplier, it is only accurate as long as the output of the divider is near the top of its range (near 10 v on this model). A voltage sensing servo system operating on the divider output and increasing the gain of amplifier No. 1 while simultaneously decreasing the gain of the follower amplifier No. 6

(or a buffer amplifier following this) would maintain the divider output high, while keeping the overall loop gain constant. For the purposes of the experiments reported in this paper, since absolute values were not needed, the additional sophistication of a constant gain servo system was not incorporated into the normalized excitation system.

As a test of the system, the same signals were introduced into both channels of the analog computer. These signals were then raised and lowered but the output of the computer was not affected. In addition, the same signal was fed to both pens of the two pen recorder in order to determine if there was any difference in response of the two recorder channels and also to determine the amount of "lead" that one pen had over the other (both pens did not travel in the same plane across the paper). In addition, known voltage ratios were fed into the divider network in order to check its operation. These results are shown in Table VII.

Prior to making a run, the outputs of both the lock-in amplifiers were checked to make sure that they ranged from +0.5 v to -0.5 v. The bucking voltage on the computer was then checked to ensure that both voltages had a range of 0 to -1.0 v, and then all of the

Table VII. Measured versus calculated quotients for analog divider.

| $I_f$, volts | $I_e$, volts | $I_f/I_e$ ±0.01v meas. | $I_f/I_e$, cal. | % error |
|---|---|---|---|---|
| 10 | 1 | 9.90 | 10 | -1 |
| 9 | 1 | 8.88 | 9 | -1.3 |
| 8 | 1 | 7.94 | 8 | -0.75 |
| 7 | 1 | 7.03 | 7 | +0.43 |
| 6 | 1 | 6.01 | 6 | +0.17 |
| 5 | 1 | 5.04 | 5 | +0.8 |
| 4 | 1 | 4.02 | 4 | +0.5 |
| 3 | 1 | 3.01 | 3 | +0.3 |
| 2 | 1 | 2.04 | 2 | +2 |
| 1 | 1 | 0.96 | 1 | -4 |
| 1 | 0.9 | 1.14 | 1.12 | +1.8 |
| 1 | 0.8 | 1.27 | 1.25 | +1.6 |
| 1 | 0.7 | 1.48 | 1.43 | +3.5 |
| 1 | 0.6 | 1.69 | 1.67 | +1.2 |
| 1 | 0.5 | 2.05 | 2.0 | +2.5 |
| 1 | 0.4 | 2.54 | 2.50 | +1.6 |
| 1 | 0.3 | 3.37 | 3.33 | +1.2 |
| 1 | 0.2 | 5.08 | 5.0 | +1.6 |

operational amplifiers in the circuit were balanced. Finally, all the recorder zeroes were checked with zero signal input. An attentuator on the output of the final operational amplifier (No. 6) was then used to fit that part of the output range desired to the single pen chart recorder.

The above method of obtaining normalized excitation spectra is similar in concept to that used by Rosen and Edelman,[46] which, in turn, is based on the earlier work of Parker,[47] who used a mechanical ratio recorder to take the ratio of the fluorescence produced in the sample to the fluorescence produced in a given reference liquid by the excitation. The accurate operation of the system depended on the choice of the reference fluorescent solution, and was restricted to a fairly narrow spectral range. It was also necessary to manually adjust the excitation monochromator slits to keep the excitation constant within a factor of two: Rosen and Edwards used the output of a photomultiplier monitoring the excitation to modify the gain of the fluorescence amplifier, and thus achieve a normalized excitation.

## LIST OF REFERENCES


1. F. Varsanyi and G. H. Dieke, Phys. Rev. Letters 7, 442 (1961).

2. G. H. Dieke and E. Dorman, Phys. Rev. Letters 11, 17 (1963).

3. G. H. Dieke, Paramagnetic Resonance, edited by W. Low, (Academic Press, New York, 1963), Vol. 1, pp. 237-252.

4. G. H. Dieke, Spectra and Energy Levels of Rare Earth Ions in Crystals, edited by H. M. Crosswhite and Hannah Crosswhite, (Interscience Publishers, New York, 1968).

5. G. E. Barasch, "Fluorescent Lifetimes of and Energy Transfer between Excited States of Rare Earth Ions in Crystals", Ph.D. Dissertation, The Johns Hopkins University, Baltimore, Maryland, 1965.

6. A. Kiel, "The Interaction of Paramagnetic Ions with Lattice Vibrations", Ph.D. Dissertation, The Johns Hopkins University, Baltimore, Maryland, 1963.

7. L. A. Riseberg and H. W. Moos, Phys. Rev. 174, 429 (1968).

8. Th. Förster, Ann. Physik 2, 55 (1948).

9. D. L. Dexter, J. Chem. Phys. 21, 836 (1953).

10. D. L. Dexter and J. H. Schulman, J. Chem. Phys. 22, 1063 (1954).

11. J. D. Dow, Phys. Rev. 174, 962 (1968).

12. R. J. Birgeneau, J. Chem. Phys. 50, 4282 (1969).

13. G. F. Imbusch, Phys. Rev. 153, 326 (1967).

14. D. L. Dexter, Phys. Rev. 126, 1962 (1962).

15. L. G. DeShazer and G. H. Dieke, J. Chem. Phys. 38, 2190 (1963).

16. G. H. Dieke and B. Pandey, J. Chem. Phys. 41, 1952 (1964).

17. J. F. Porter, Jr., "Energy Transfer between Excited States of $Ho^{3+}$ in $LaCl_3$", Ph.D. Dissertation, The Johns Hopkins University, Baltimore, Maryland, 1966.

18. J. F. Porter, Jr. and H. W. Moos, Phys. Rev. 152, 300 (1966).

19. G. E. Peterson and P. M. Bridenbaugh, J. Opt. Soc. Am. 52, 1079 (1962).

20. G. E. Peterson and P. M. Bridenbaugh, J. Opt. Soc. Am. 53, 301 (1963).

21. G. E. Peterson and P. M. Bridenbaugh, J. Opt. Soc. Am. 53, 494 (1963).

22. G. E. Peterson and P. M. Bridenbaugh, J. Opt. Soc. Am. 53, 1129 (1963).

23. G. E. Peterson and P. M. Bridenbaugh, J. Opt. Soc. Am. 54, 644 (1964).

24. J. D. Axe and P. F. Weller, J. Chem. Phys. 40, 3066 (1964).

25. J. Murphy, R. C. Ohlmann, and R. Mazelsky, Phys. Rev. Letters 13, 135 (1964).

26. Z. J. Kiss, Phys. Rev. Letters 13, 654 (1964).

27. W. M. Yen, R. L. Greene, W. C. Scott, and D. L. Huber, Phys. Rev. 140, A1188 (1965).

28. B. R. Malhotra and D. R. Bhawalkar, Indian J. Pure Appl. Phys. 7, 573 (1969).

29. N. S. Belokrinitskii, M. E. Zhabotinskii, A. D. Manuil'skii, Yu. P. Rudnitskii, M. S. Soskin, V. V. Tsapkin, and G. V. Ellert, Soviet Physics-Doklady 14, 276 (1969).

30. J. P. van der Ziel and L. G. Van Uitert, Phys. Rev. Letters 21, 1334 (1968).

31. J. P. van der Ziel and L. G. Van Uitert, Phys. Rev. 180, 343 (1969).

32. J. S. Margolis, O. Stafsudd, and E. Y. Wong, J. Chem. Phys. 38, 2045 (1963).

33. R. Sarup and M. H. Crozier, J. Chem. Phys. 42, 371 (1965).

34. G. H. Dieke and R. Sarup, J. Chem. Phys. 29, 741 (1958).

35. E. H. Carlson and G. H. Dieke, J. Chem. Phys. 29, 229 (1958).

36. E. H. Carlson and G. H. Dieke, J. Chem. Phys. 34, 1602 (1961).

37. F. Varsanyi and G. H. Dieke, J. Chem. Phys. 36, 385 (1962).

38. G. H. Dieke and B. Pandey, Proc. Symp. Optical Masers, Polytechnic Institute of Brooklyn, April 1963, p. 332.

39. J. C. Edwards and J. F. Porter, Jr., Bull. Am. Phys. Soc. 13, 1721 (1968).

40. J. C. Edwards, "Visible Continuum Radiation from Monochromatically Excited Alkali Halides", M. S. Thesis, The University of Alabama, University, Alabama, 1968.

41. R. Sarup, "Fluorescence and Absorption Spectra and Zeeman Effects of Praseodymium and Thulium Salts at 77°K and 4°K", Ph.D. Dissertation, The Johns Hopkins University, Baltimore, Maryland, 1959.

42. H. W. Moos, Optical Properties of Ions in Crystals, edited by H. M. Crosswhite and H. W. Moos (Interscience Publishers, New York, 1967), p. vii.

43. E. H. Carlson, "Absorption and Fluorescence Spectra of $NdCl_3$ and States of the Neodymium Ion", Ph.D. Dissertation, The Johns Hopkins University, Baltimore, Maryland, 1960.

44. C. A. Hutchisson and E. Y. Wong, J. Chem. Phys. 29, 754 (1958).

45. J. F. Porter, Jr., and J. H. Blatt, Physics Letters 30A, 451 (1969).

46. P. Rosen and G. M. Edelman, Rev. Sci. Inst. 36, 809 (1965).

47. C. A. Parker, Nature 182, 1002 (1958).